Supplement of Atmos. Chem. Phys., 18, 8757–8787, 2018
https://doi.org/10.5194/acp-18-8757-2018-supplement

Atmospheric Chemistry and Physics
Open Access
EGU

Supplement of

Direct radiative effects during intense Mediterranean desert dust outbreaks

Antonis Gkikas et al.

Correspondence to: Antonis Gkikas (agkikas@noa.gr)

	MODIS-Terra (AOD at 550nm)	NMMB-MONARCH (AOD at 550nm)
31 Jul 2001	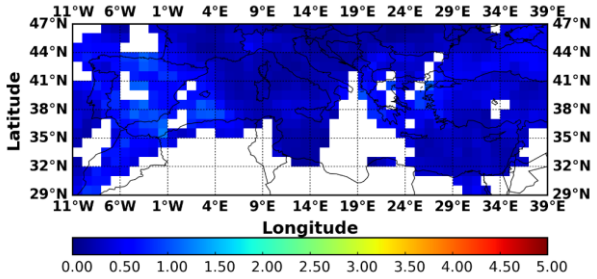	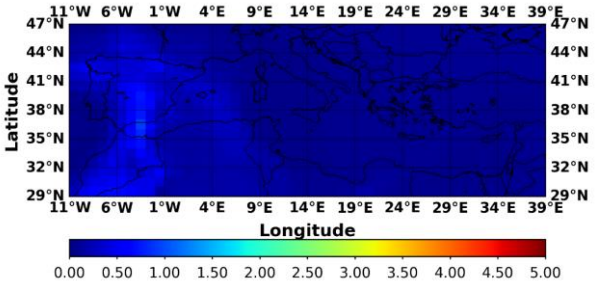
8 May 2002	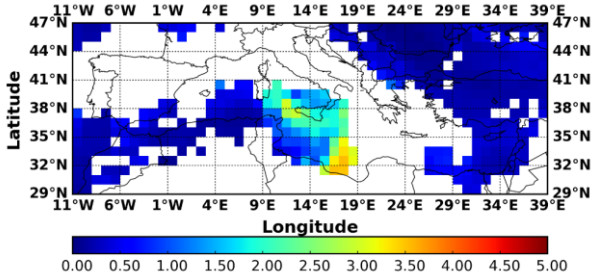	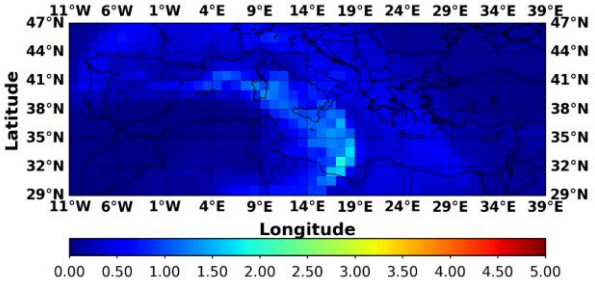
4 Apr 2003	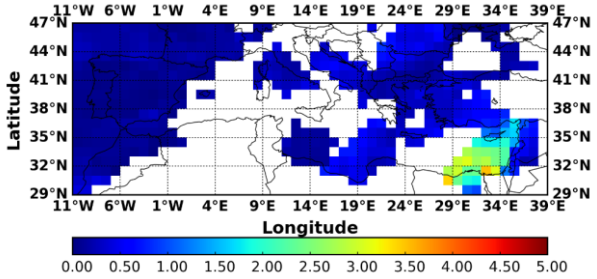	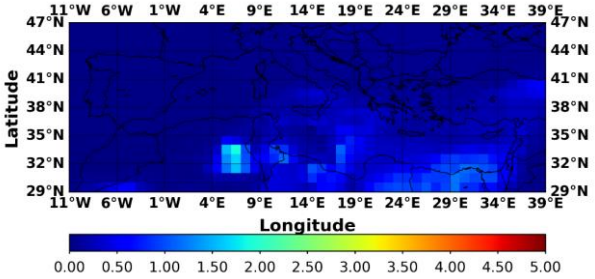
16 Jul 2003	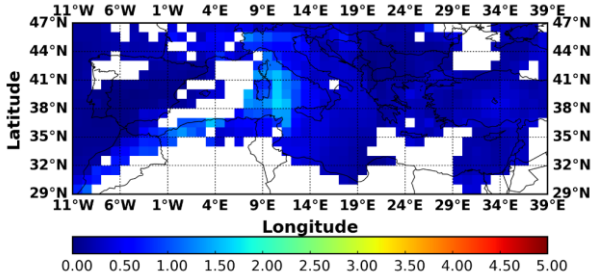	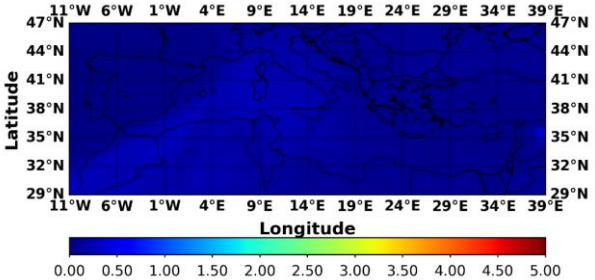
22 Feb 2004	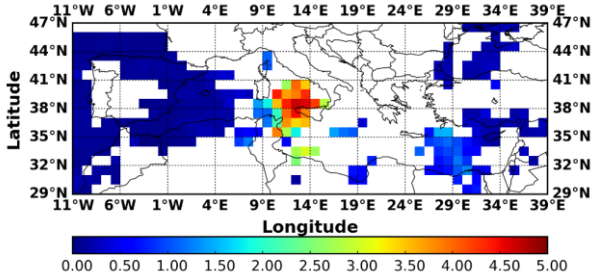	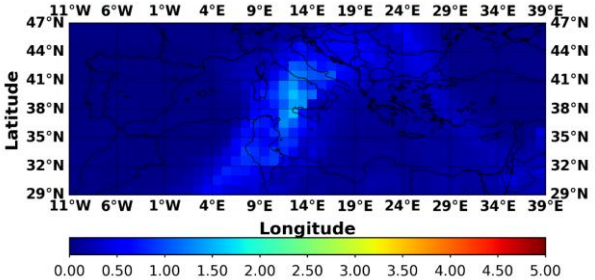
26 Mar 2004	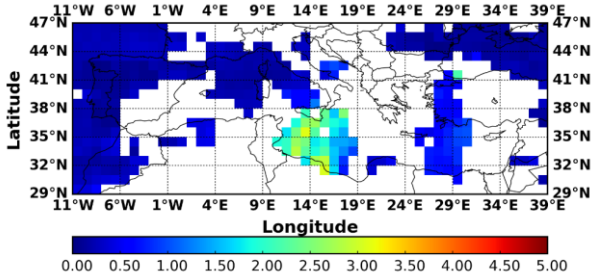	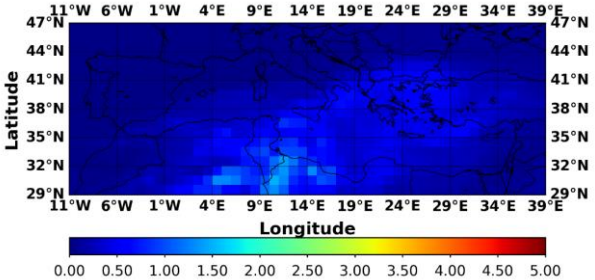

27 Jan 2005

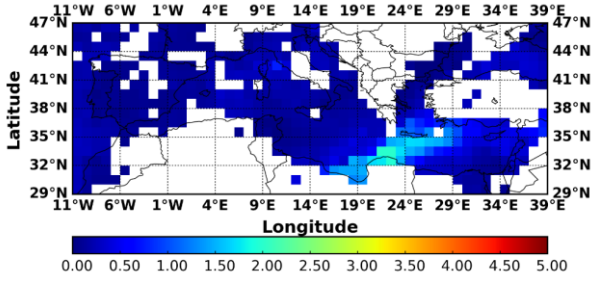

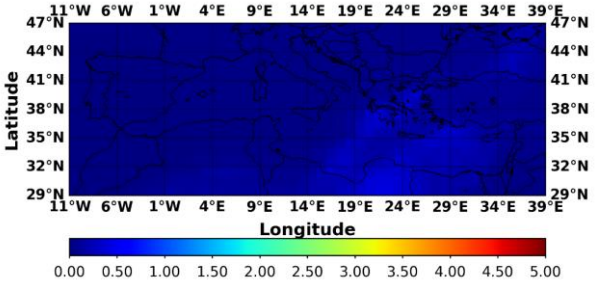

28 Jul 2005

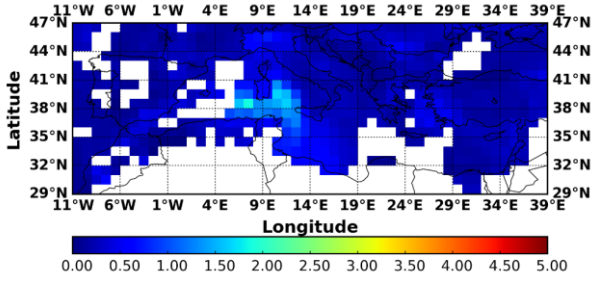

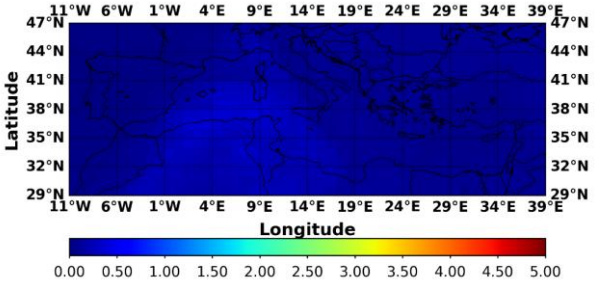

24 Feb 2006

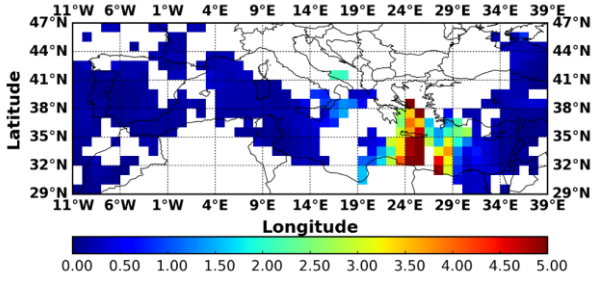

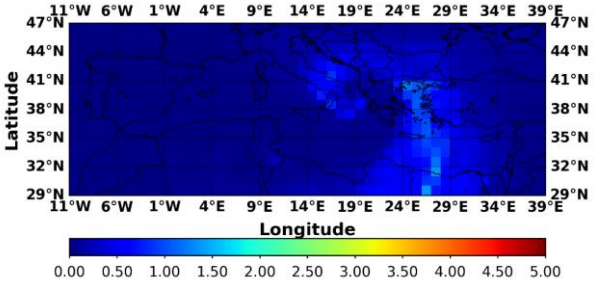

19 Mar 2006

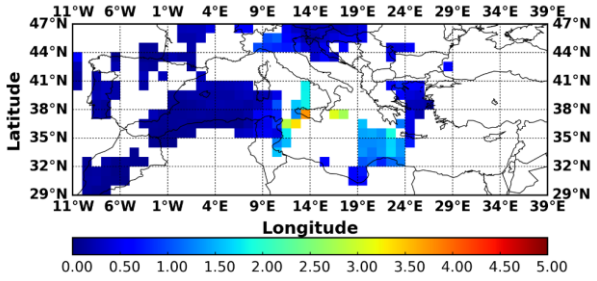

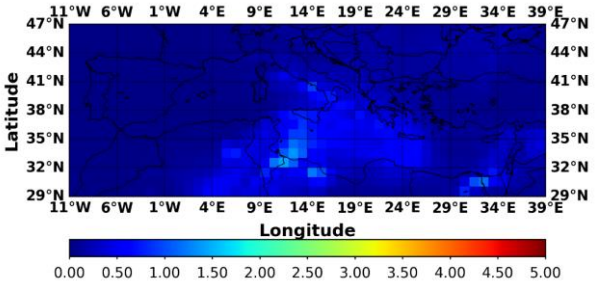

24 Feb 2007

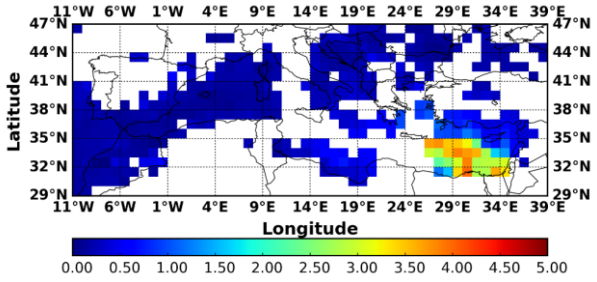

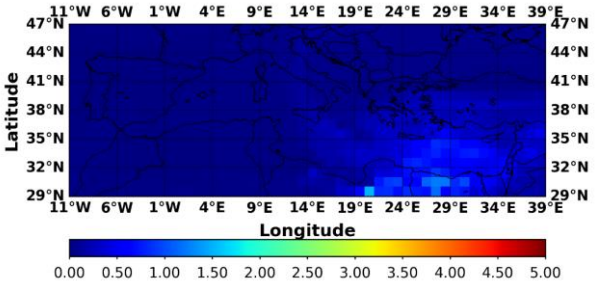

21 Apr 2007

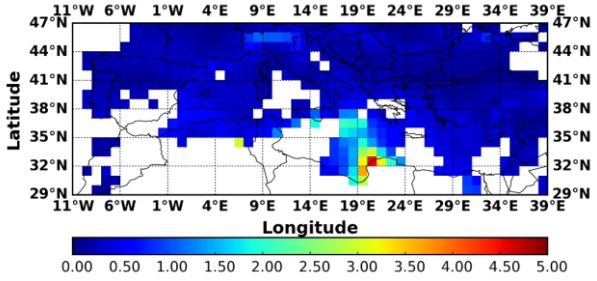

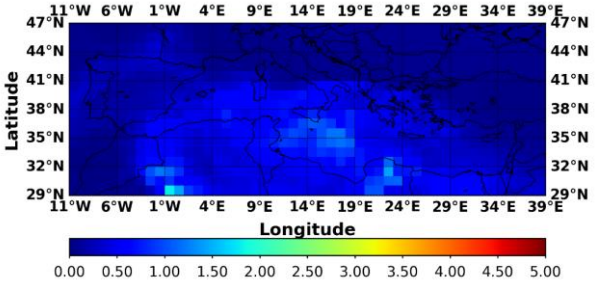

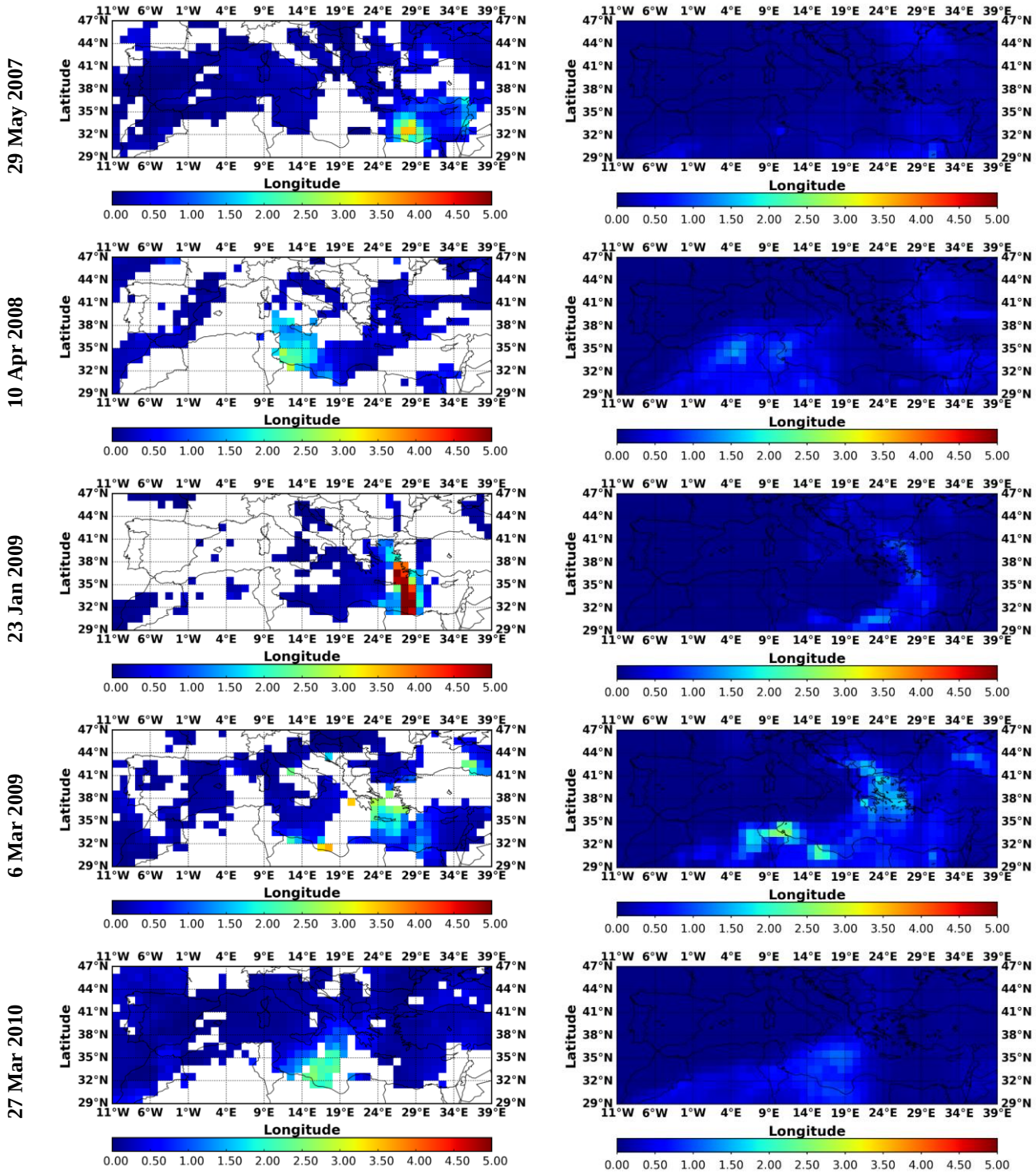

Figure S1: Geographical distributions of the daily MODIS-Terra AOD at 550nm (left column) and the simulated AOD at 550nm at 12:00 UTC (right column) for the Mediterranean desert dust outbreaks that took place on 31st July 2001, 8th May 2002, 4th April 2003, 16th July 2003, 22nd February 2004, 26th March 2004, 27th January 2005, 28th July 2005, 24th February 2006, 19th March 2006, 24th February 2007, 21st April 2007, 29th May 2007, 10th April 2008, 23rd January 2009, 6th March 2009 and 27th March 2010.

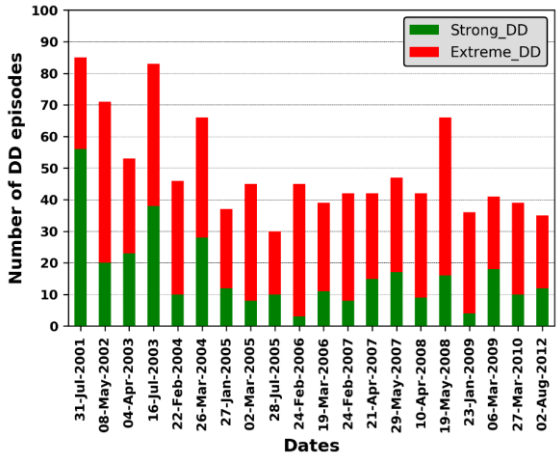

(i)

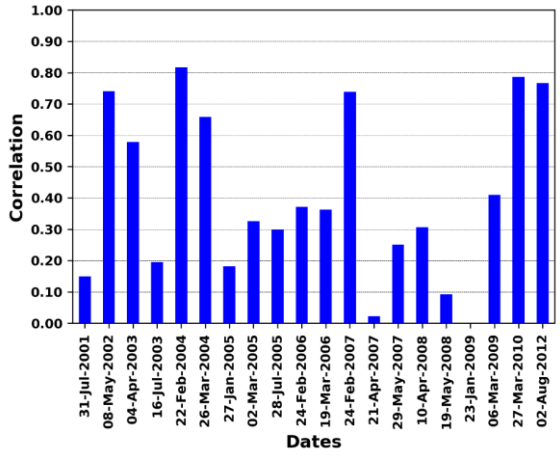

(ii)

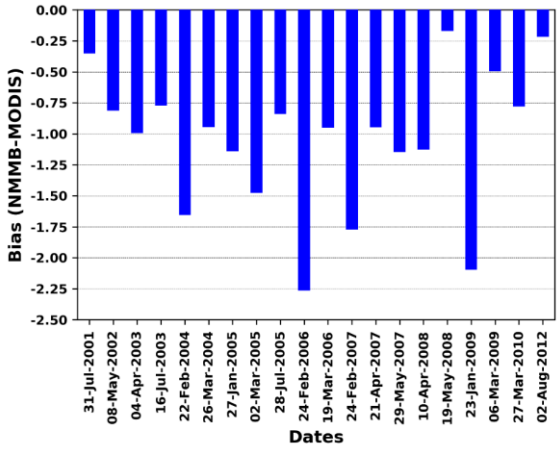

(iii)

Figure S2: (i) Number of strong (green bars), extreme (red bars) and total (height of bars) DD episodes identified by the satellite algorithm, (ii) Correlation coefficients (R) calculated between satellite AODs and model dust AODs, (iii) Regional biases (defined as NMMB-MODIS) between the simulated and the retrieved AODs. The obtained results are presented for each date (x axis) and for their derivation have been taken into account only the pixels where a DD episode (either strong or extreme) has been identified by the satellite algorithm.

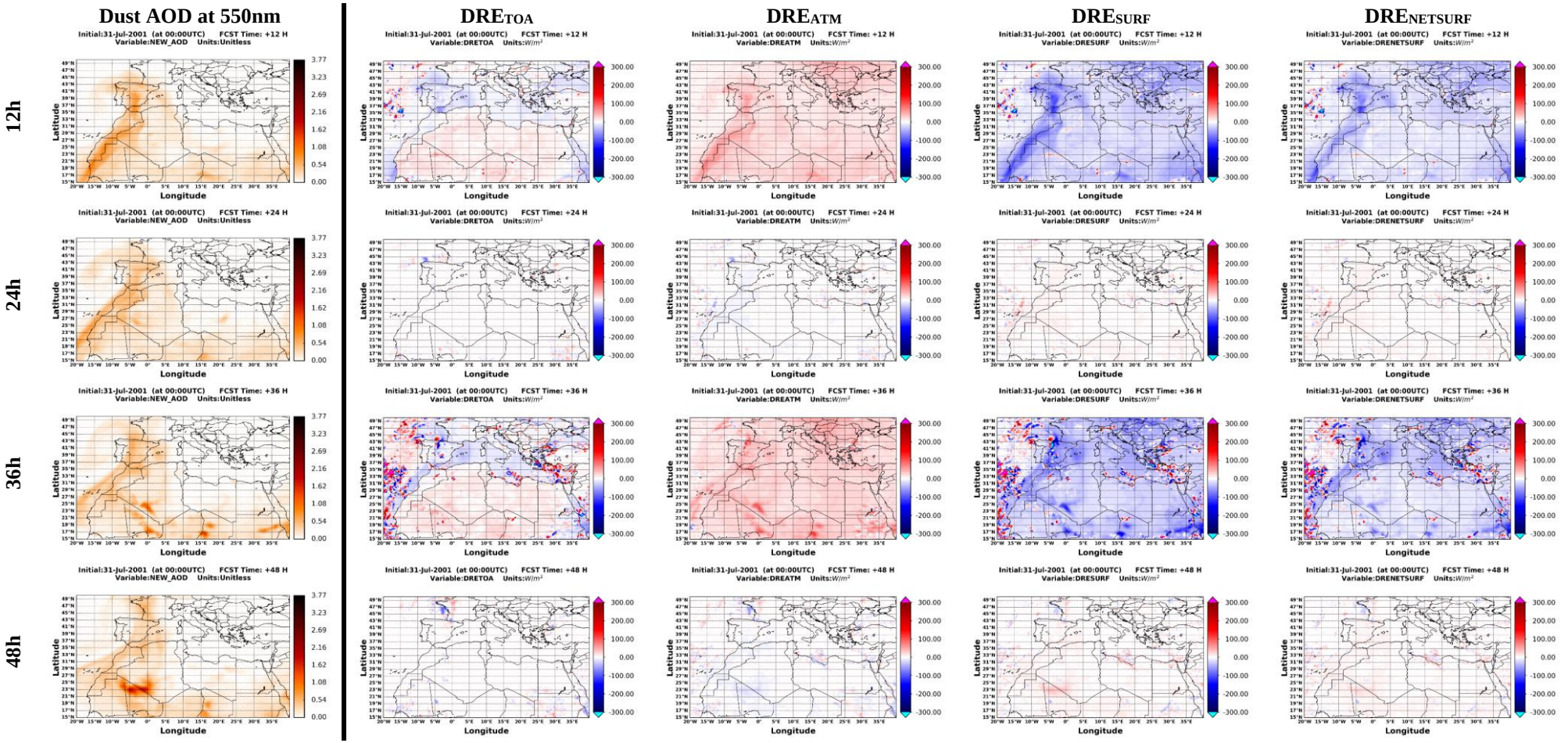

Figure S3: Spatial patterns of the simulated dust AOD_{550nm} and the instantaneous DRE_{TOA}, DRE_{ATM}, DRE_{SURF} and $DRE_{NETSURF}$ values, expressed in Wm^{-2}, at 12, 24, 36 and 48 hours after the initialization of NMMB-MONARCH model at 00 UTC on 31st July 2001.

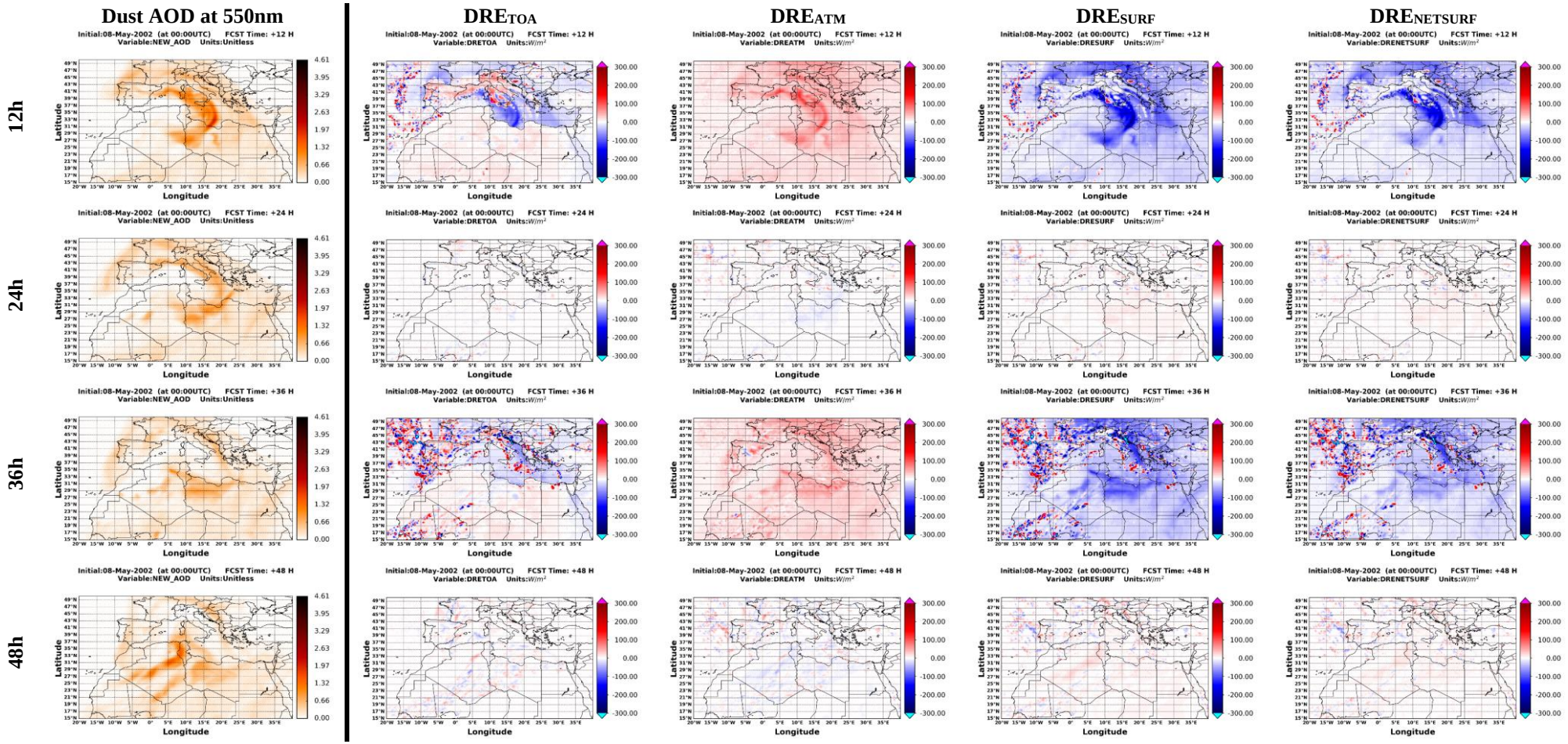

Figure S4: Spatial patterns of the simulated dust AOD_{550nm} and the instantaneous DRE_{TOA}, DRE_{ATM}, DRE_{SURF} and $DRE_{NETSURF}$ values, expressed in Wm^{-2}, at 12, 24, 36 and 48 hours after the initialization of NMMB-MONARCH model at 00 UTC on 8th May 2002.

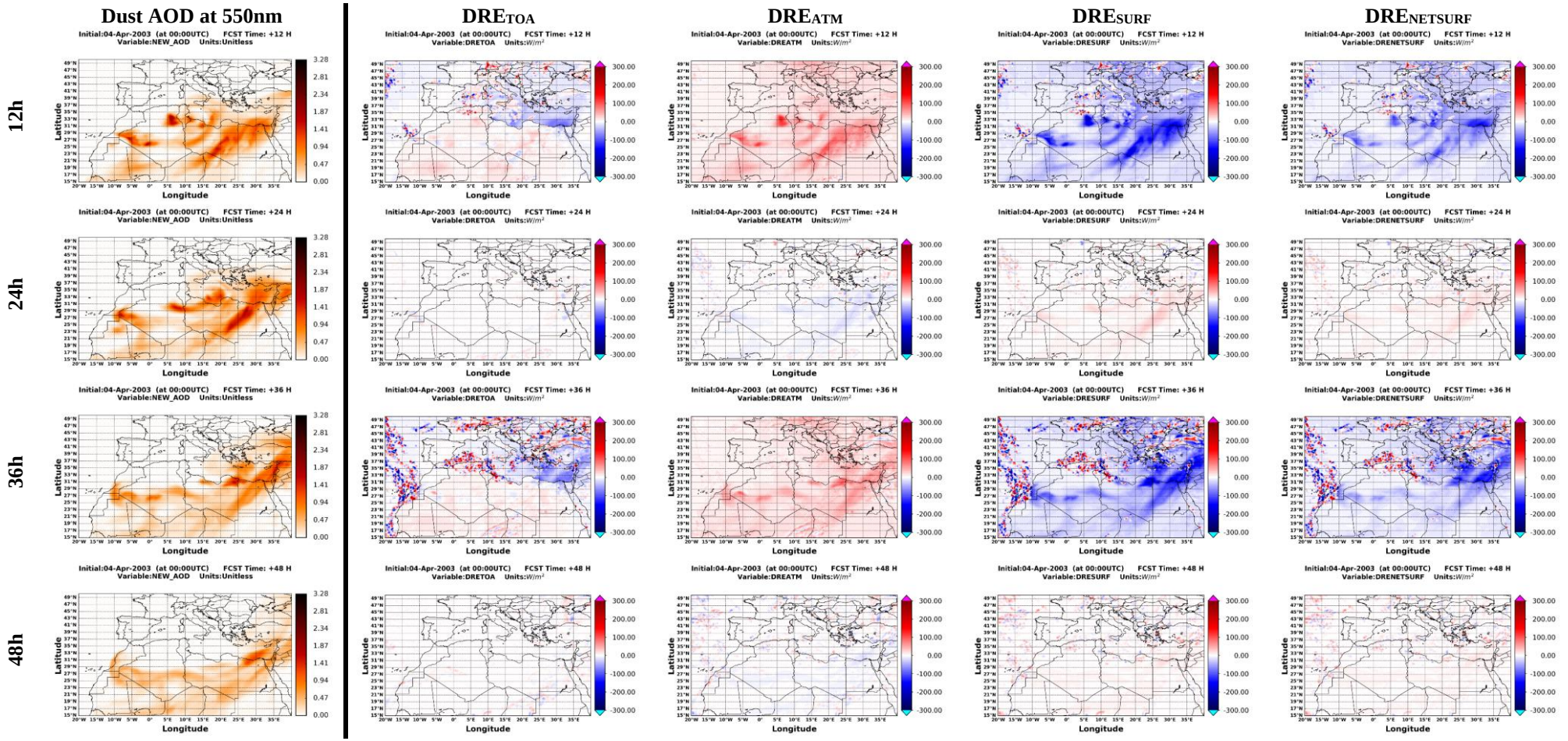

Figure S5: Spatial patterns of the simulated dust AOD_{550nm} and the instantaneous DRE_{TOA}, DRE_{ATM}, DRE_{SURF} and $DRE_{NETSURF}$ values, expressed in Wm^{-2}, at 12, 24, 36 and 48 hours after the initialization of NMMB-MONARCH model at 00 UTC on 4th April 2003.

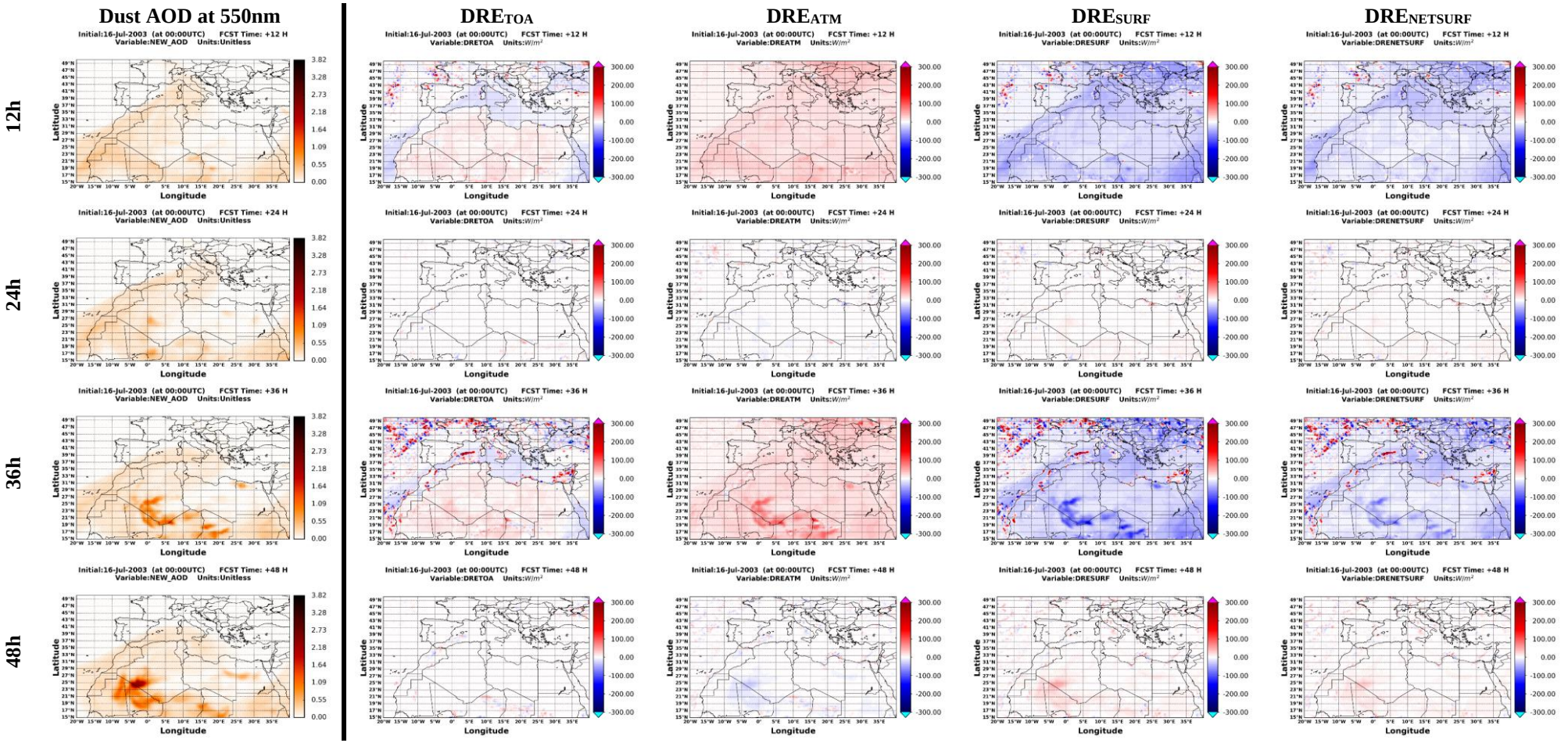

Figure S6: Spatial patterns of the simulated dust AOD_{550nm} and the instantaneous DRE_{TOA}, DRE_{ATM}, DRE_{SURF} and $DRE_{NETSURF}$ values, expressed in Wm^{-2}, at 12, 24, 36 and 48 hours after the initialization of NMMB-MONARCH model at 00 UTC on 16th July 2003.

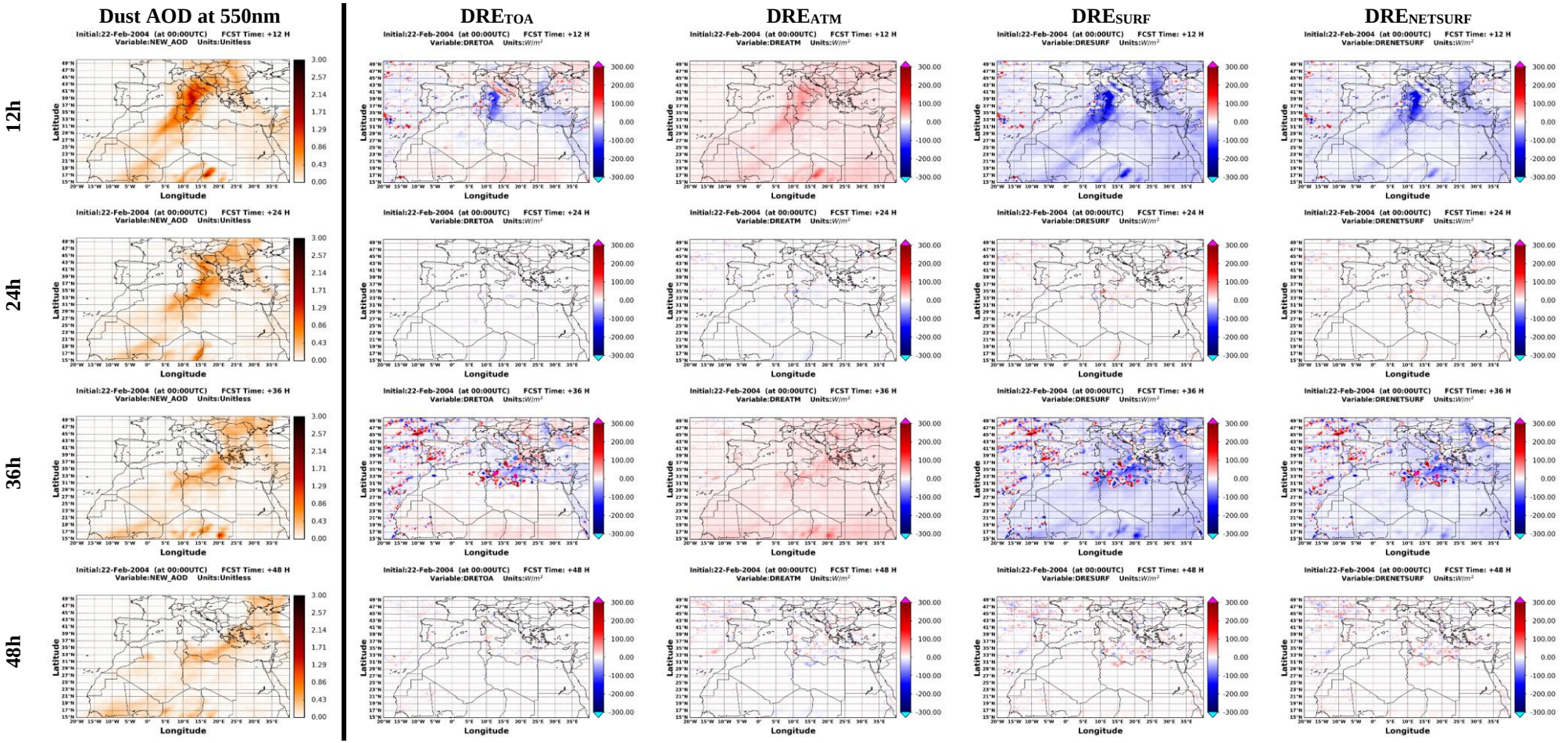

Figure S7: Spatial patterns of the simulated dust AOD_{550nm} and the instantaneous DRE_{TOA}, DRE_{ATM}, DRE_{SURF} and $DRE_{NETSURF}$ values, expressed in Wm^{-2}, at 12, 24, 36 and 48 hours after the initialization of NMMB-MONARCH model at 00 UTC on 22nd February 2004.

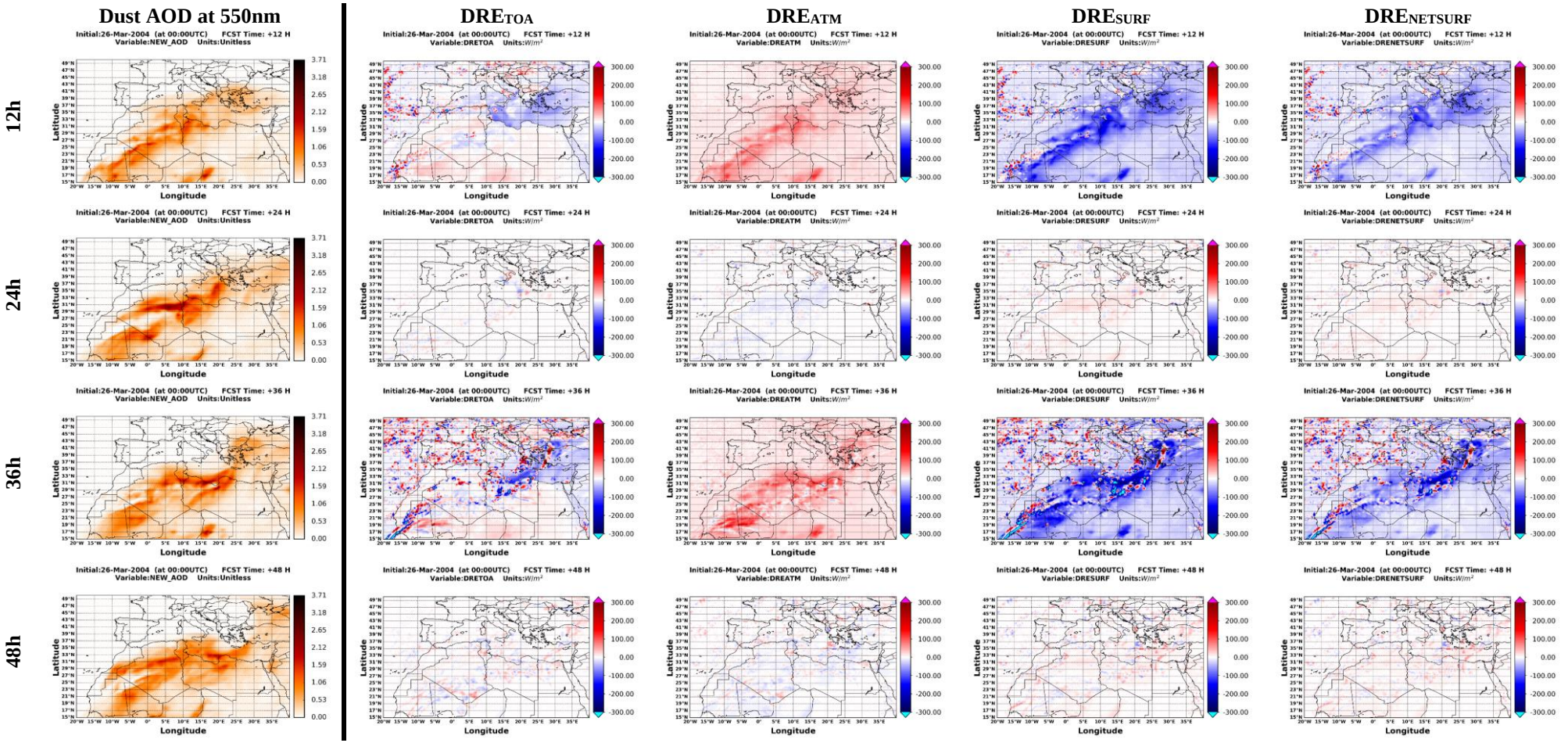

Figure S8: Spatial patterns of the simulated dust AOD_{550nm} and the instantaneous DRE_{TOA}, DRE_{ATM}, DRE_{SURF} and $DRE_{NETSURF}$ values, expressed in Wm^{-2}, at 12, 24, 36 and 48 hours after the initialization of NMMB-MONARCH model at 00 UTC on 26th March 2004.

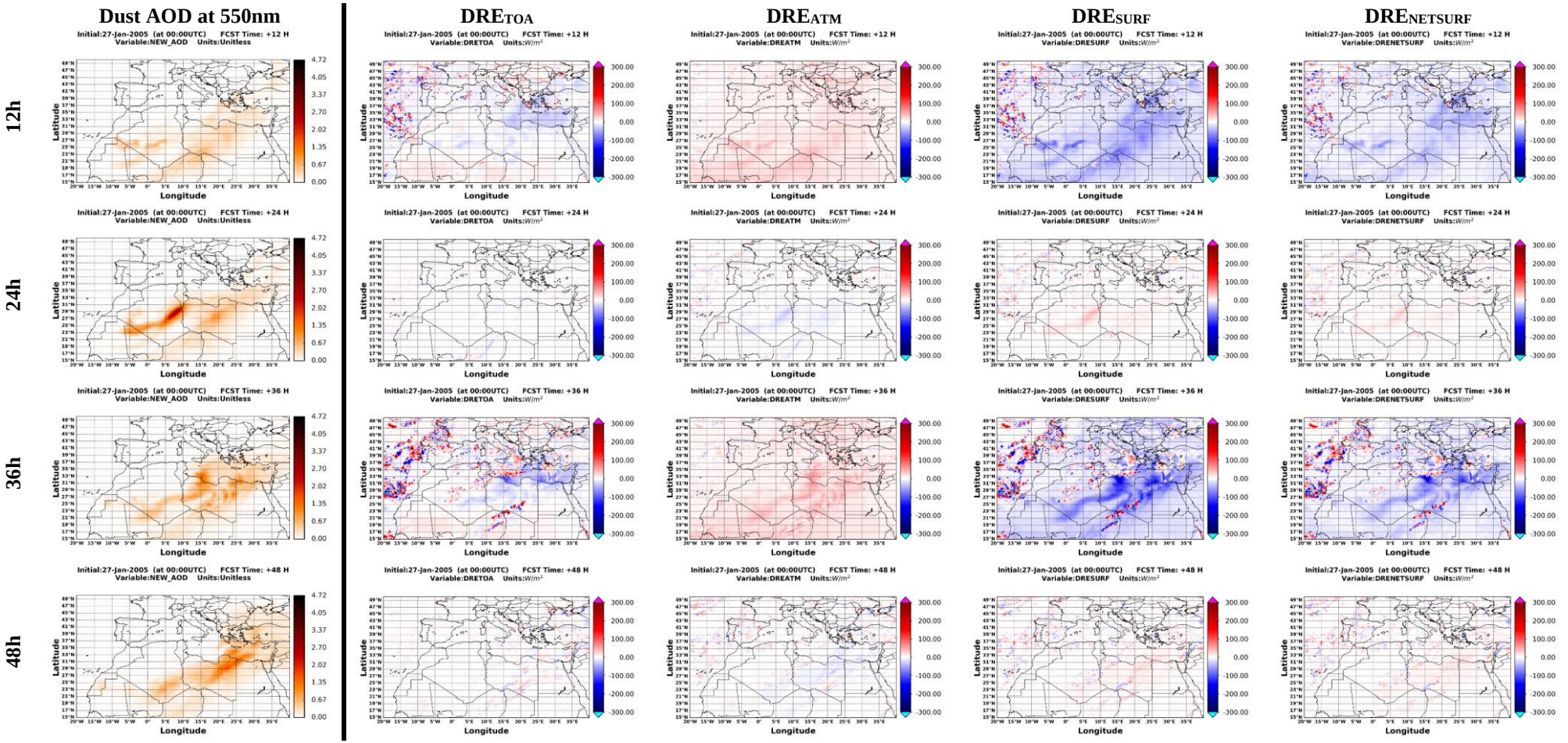

Figure S9: Spatial patterns of the simulated dust AOD_{550nm} and the instantaneous DRE_{TOA}, DRE_{ATM}, DRE_{SURF} and $DRE_{NETSURF}$ values, expressed in Wm^{-2}, at 12, 24, 36 and 48 hours after the initialization of NMMB-MONARCH model at 00 UTC on 27th January 2005.

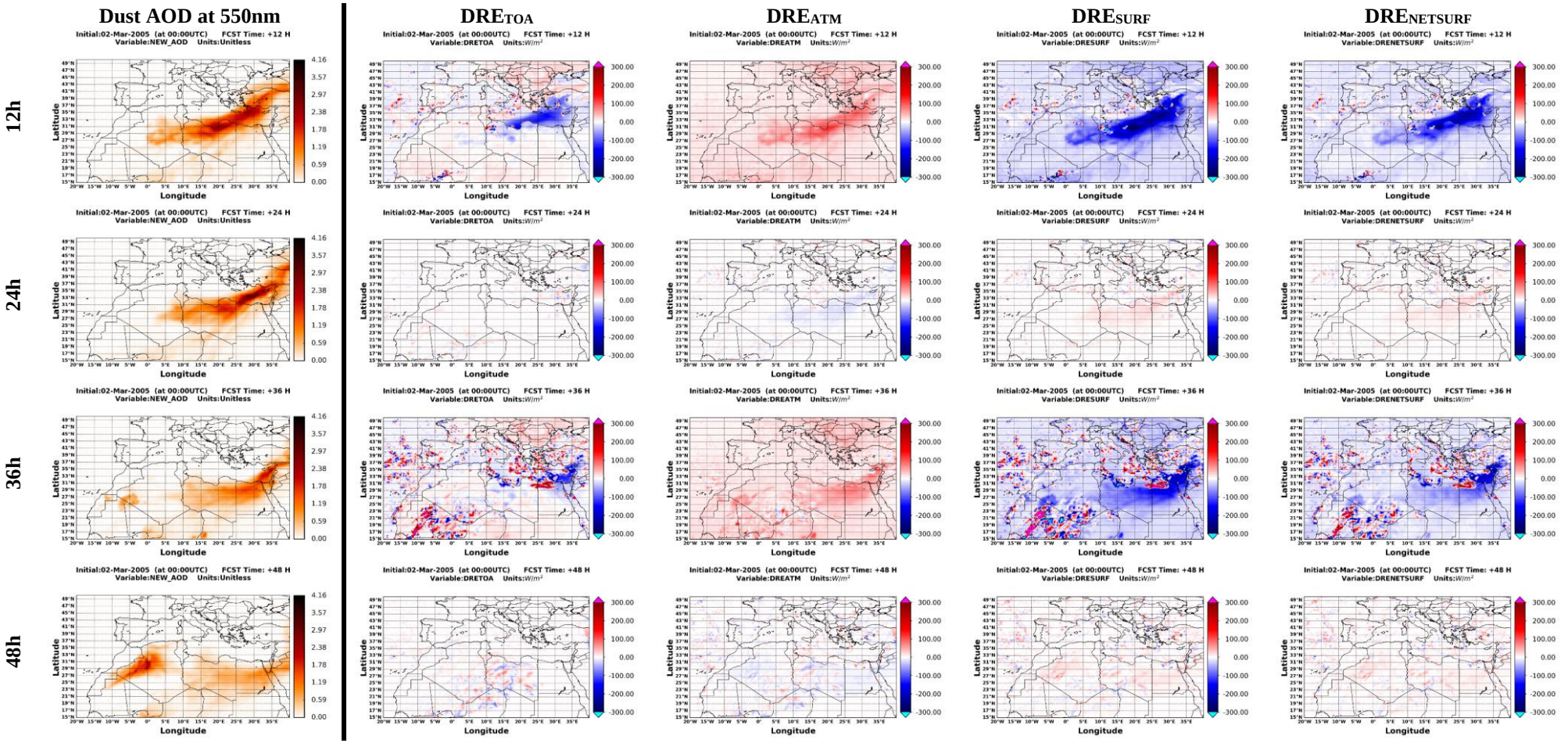

Figure S10: Spatial patterns of the simulated dust AOD_{550nm} and the instantaneous DRE_{TOA}, DRE_{ATM}, DRE_{SURF} and $DRE_{NETSURF}$ values, expressed in Wm^{-2}, at 12, 24, 36 and 48 hours after the initialization of NMMB-MONARCH model at 00 UTC on 2nd March 2005.

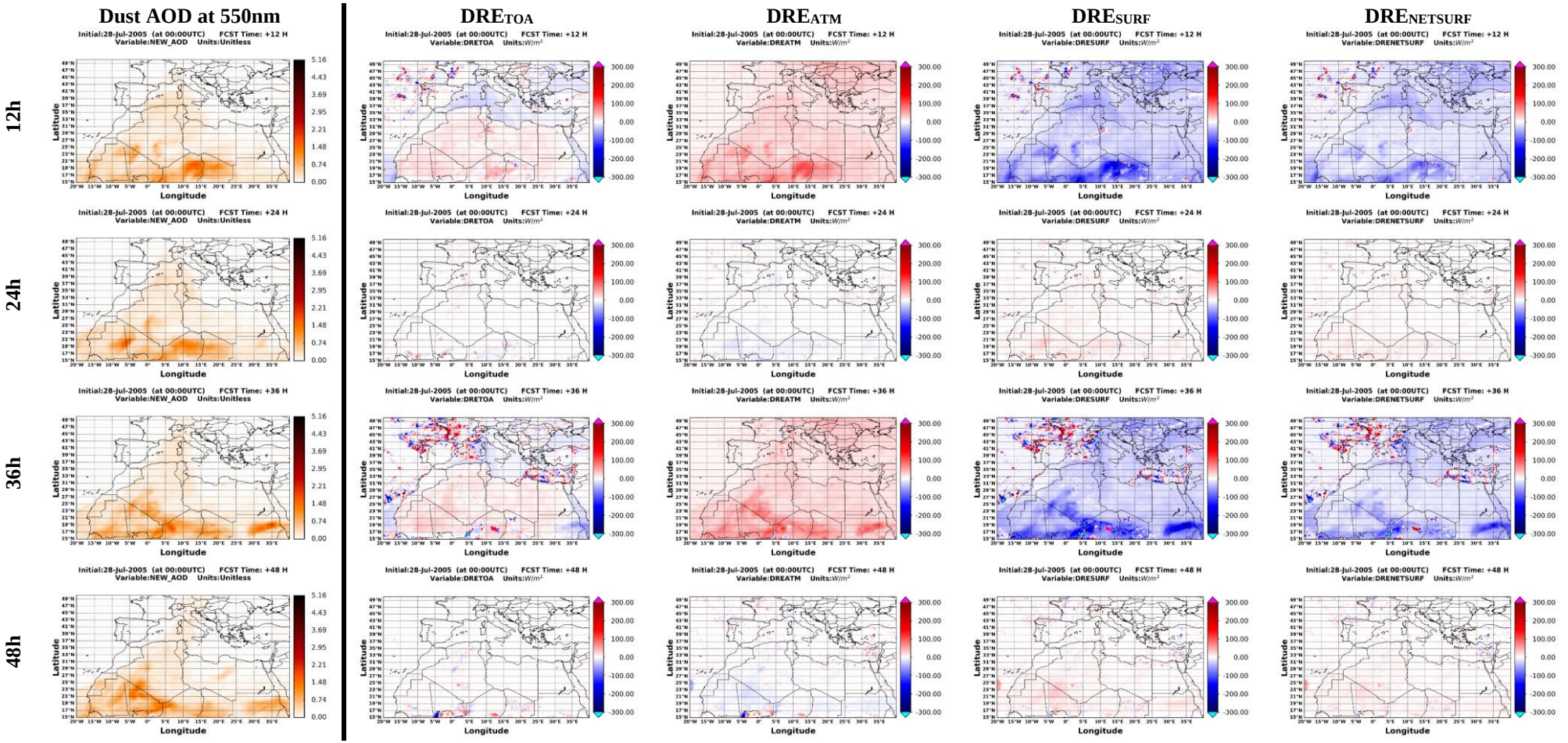

Figure S11: Spatial patterns of the simulated dust AOD_{550nm} and the instantaneous DRE_{TOA}, DRE_{ATM}, DRE_{SURF} and $DRE_{NETSURF}$ values, expressed in Wm^{-2}, at 12, 24, 36 and 48 hours after the initialization of NMMB-MONARCH model at 00 UTC on 28th July 2005.

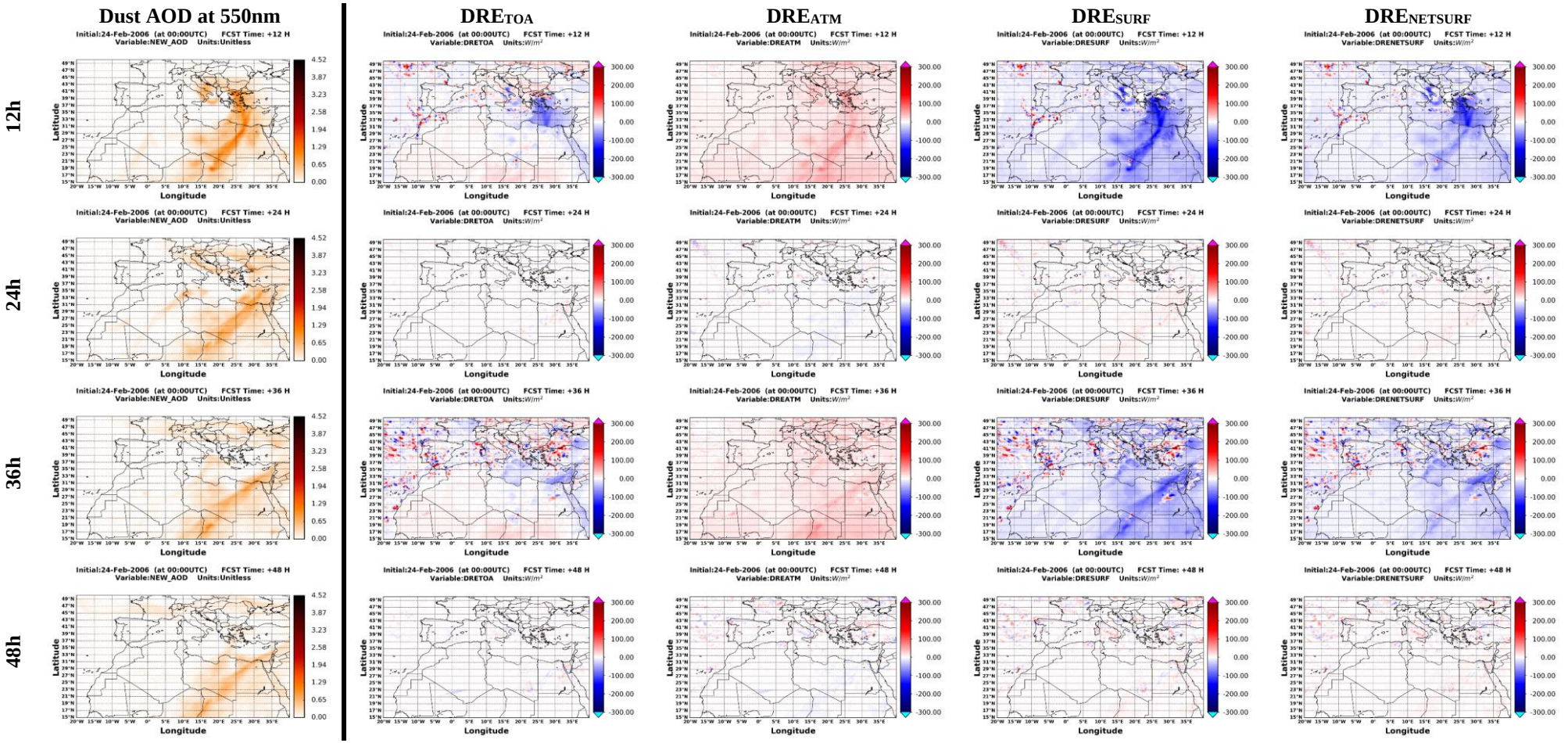

Figure S12: Spatial patterns of the simulated dust AOD_{550nm} and the instantaneous DRE_{TOA}, DRE_{ATM}, DRE_{SURF} and $DRE_{NETSURF}$ values, expressed in Wm^{-2}, at 12, 24, 36 and 48 hours after the initialization of NMMB-MONARCH model at 00 UTC on 24th February 2006.

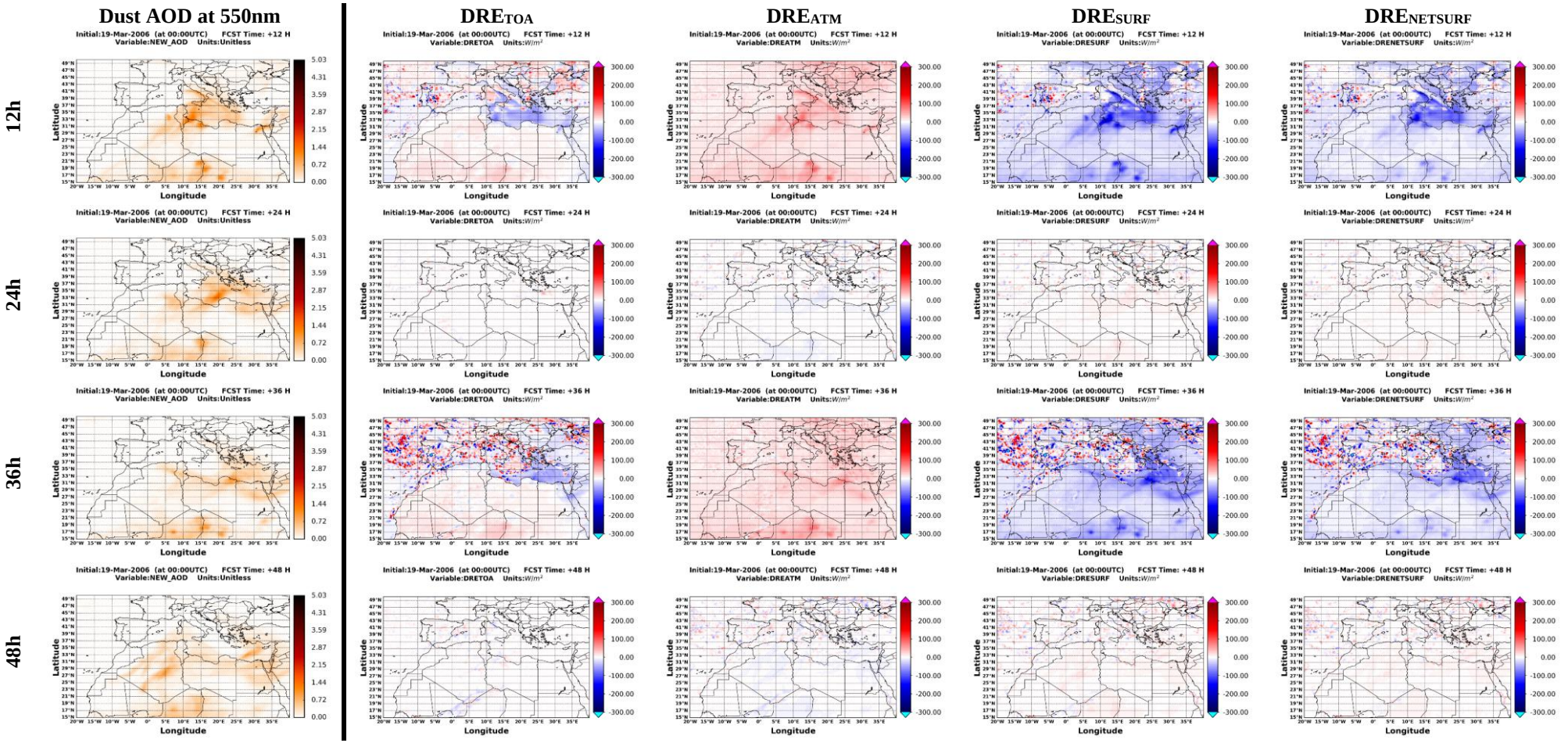

Figure S13: Spatial patterns of the simulated dust AOD_{550nm} and the instantaneous DRE_{TOA}, DRE_{ATM}, DRE_{SURF} and $DRE_{NETSURF}$ values, expressed in Wm^{-2}, at 12, 24, 36 and 48 hours after the initialization of NMMB-MONARCH model at 00 UTC on 19th March 2006.

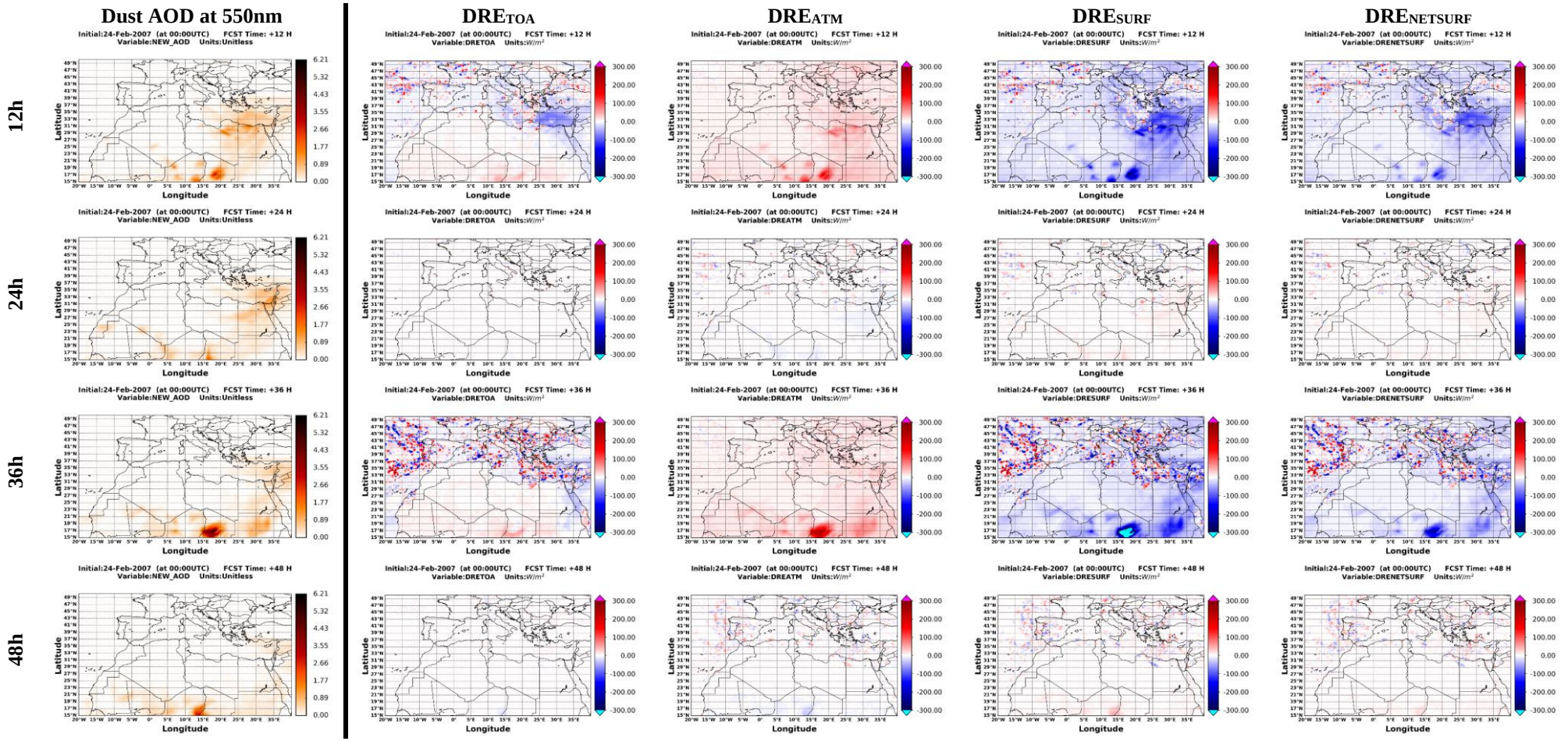

Figure S14: Spatial patterns of the simulated dust AOD_{550nm} and the instantaneous DRE_{TOA}, DRE_{ATM}, DRE_{SURF} and $DRE_{NETSURF}$ values, expressed in Wm^{-2}, at 12, 24, 36 and 48 hours after the initialization of NMMB-MONARCH model at 00 UTC on 24th February 2007.

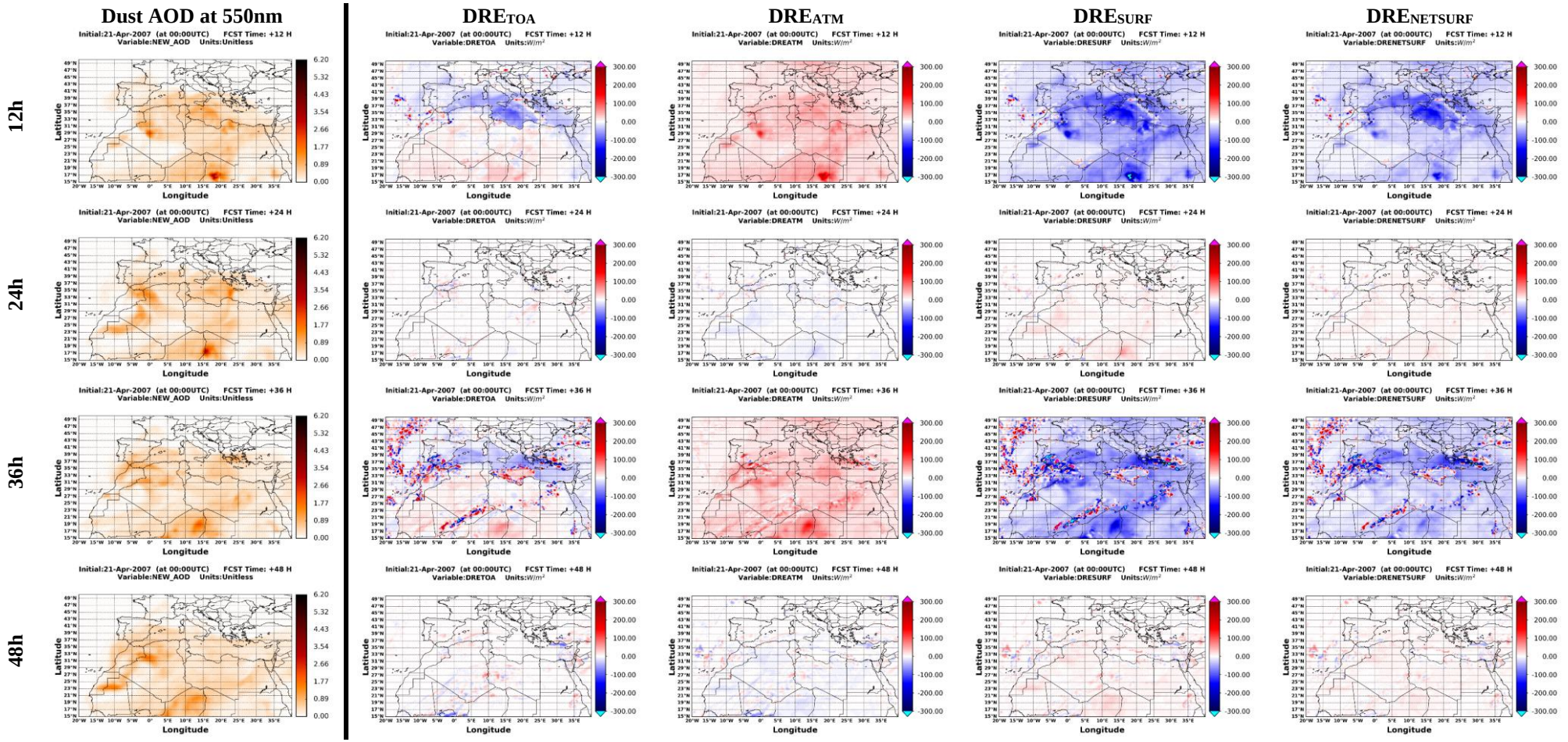

Figure S15: Spatial patterns of the simulated dust AOD_{550nm} and the instantaneous DRE_{TOA}, DRE_{ATM}, DRE_{SURF} and $DRE_{NETSURF}$ values, expressed in Wm^{-2}, at 12, 24, 36 and 48 hours after the initialization of NMMB-MONARCH model at 00 UTC on 21st April 2007.

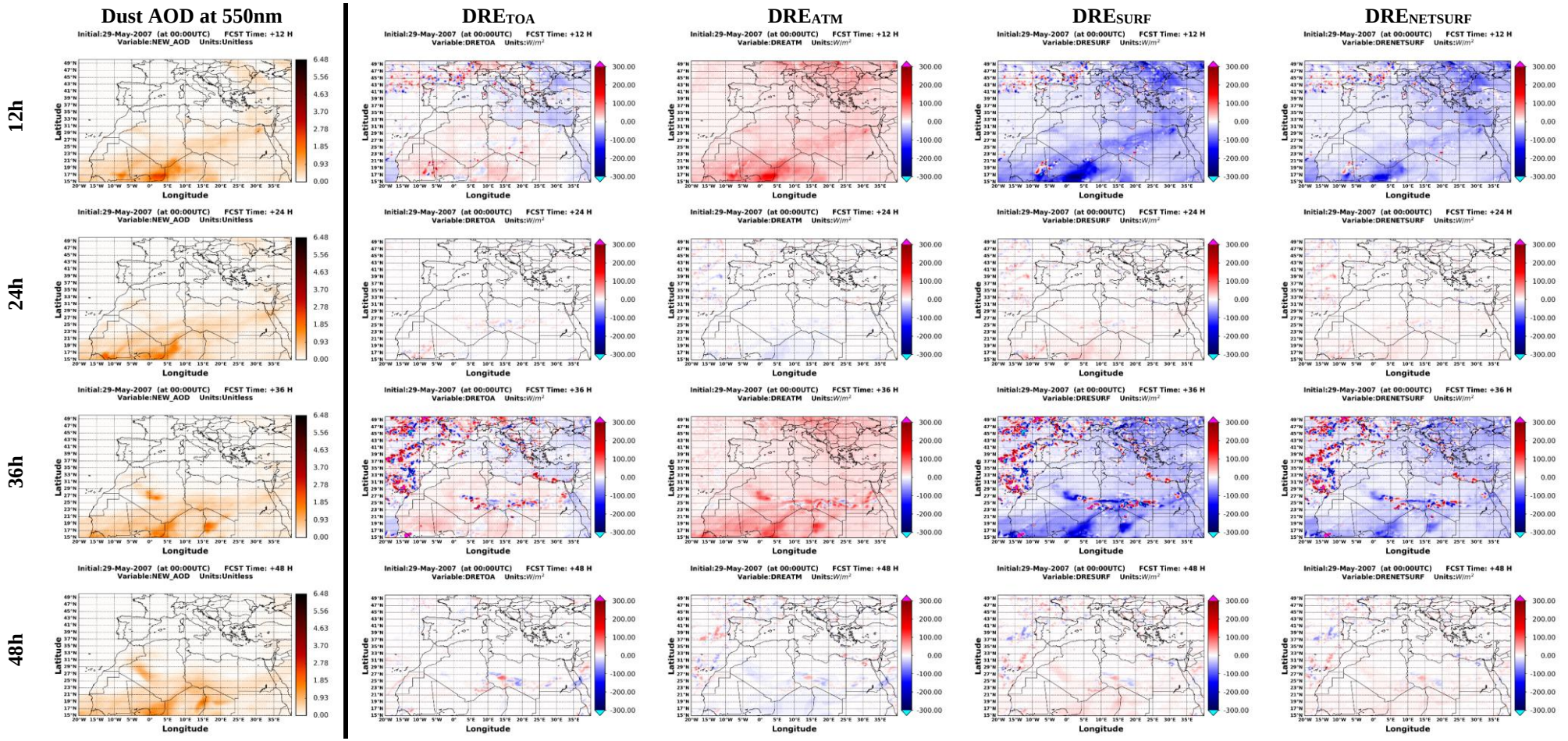

Figure S16: Spatial patterns of the simulated dust AOD_{550nm} and the instantaneous DRE_{TOA}, DRE_{ATM}, DRE_{SURF} and $DRE_{NETSURF}$ values, expressed in Wm^{-2}, at 12, 24, 36 and 48 hours after the initialization of NMMB-MONARCH model at 00 UTC on 29th May 2007.

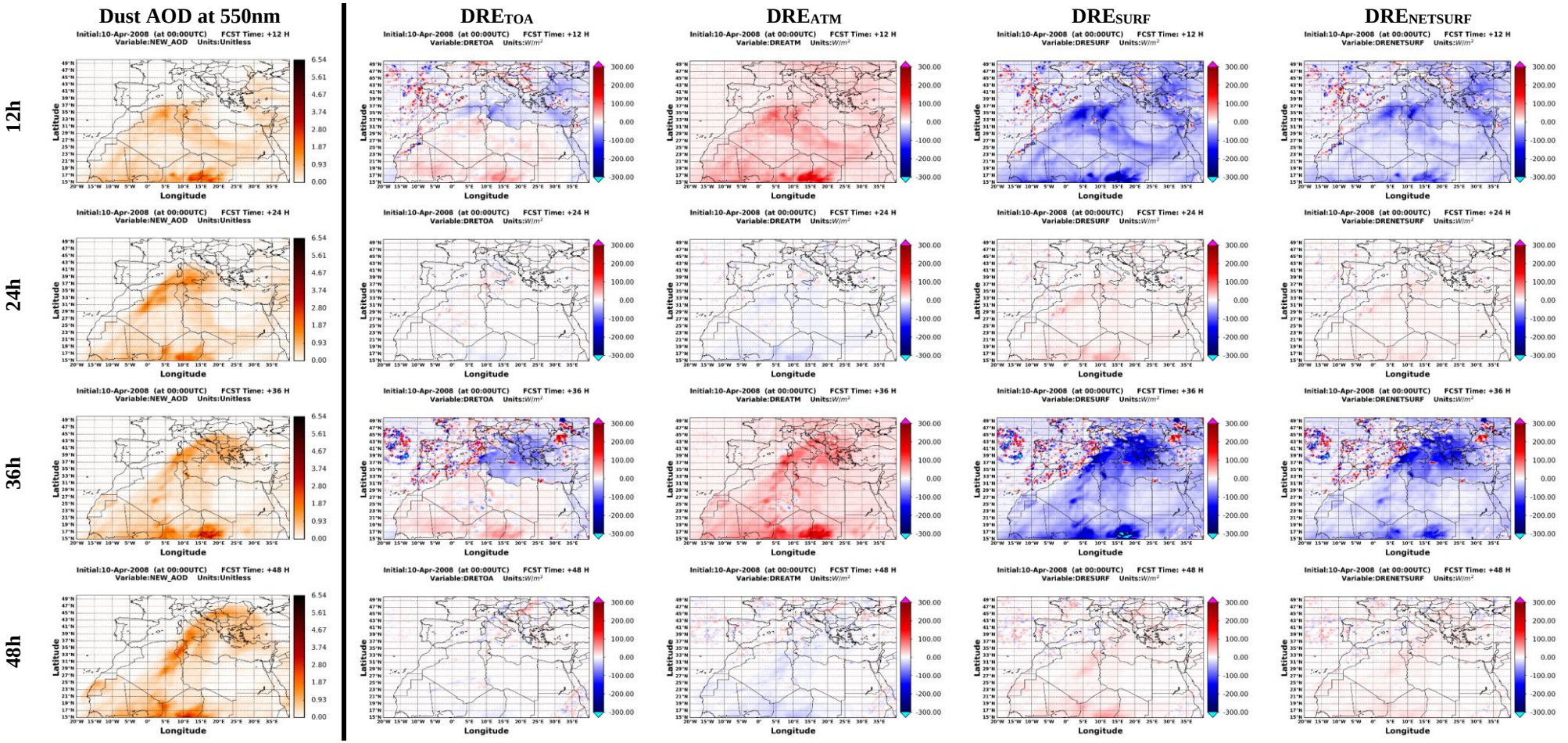

Figure S17: Spatial patterns of the simulated dust AOD_{550nm} and the instantaneous DRE_{TOA}, DRE_{ATM}, DRE_{SURF} and $DRE_{NETSURF}$ values, expressed in Wm^{-2}, at 12, 24, 36 and 48 hours after the initialization of NMMB-MONARCH model at 00 UTC on 10th April 2008.

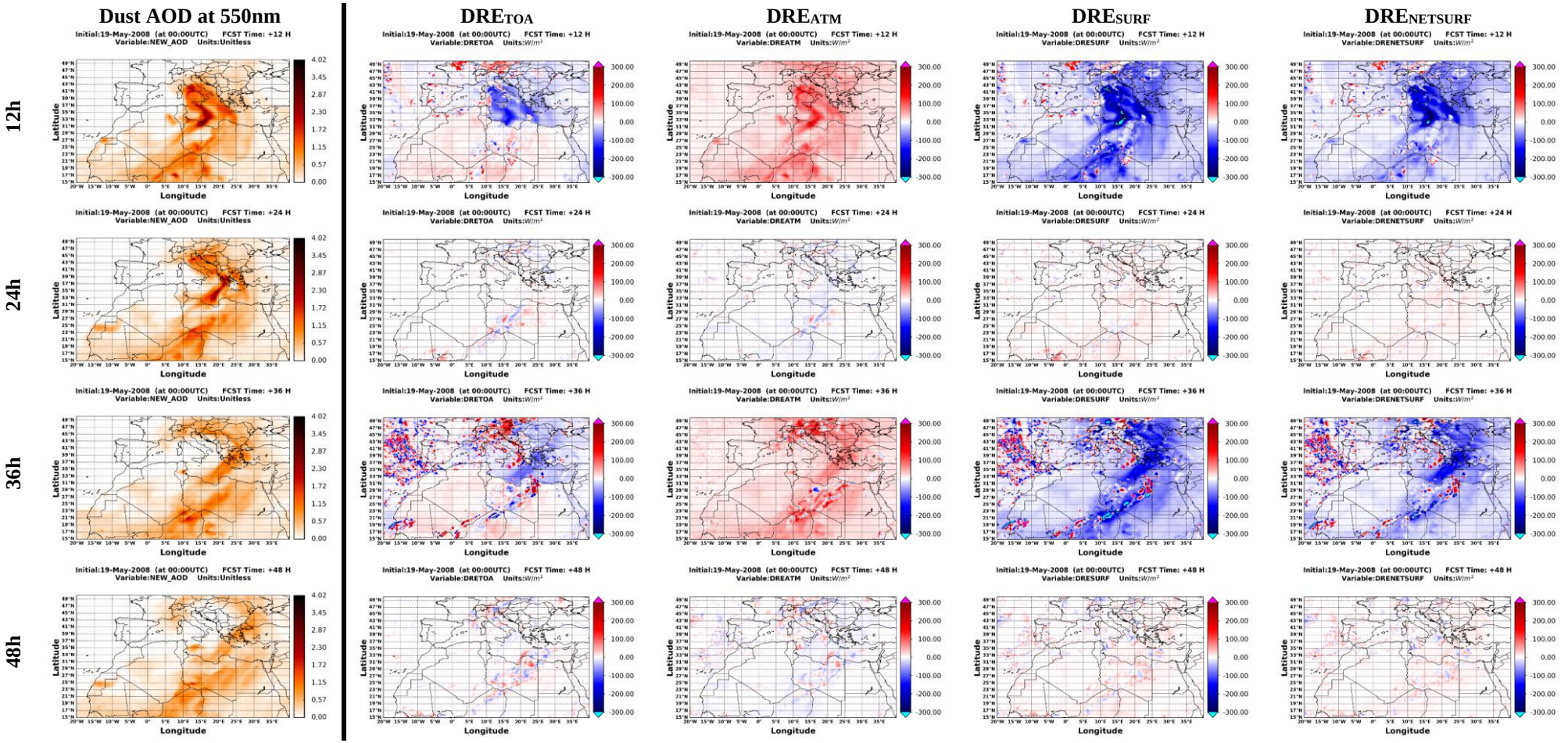

Figure S18: Spatial patterns of the simulated dust AOD_{550nm} and the instantaneous DRE_{TOA}, DRE_{ATM}, DRE_{SURF} and $DRE_{NETSURF}$ values, expressed in Wm^{-2}, at 12, 24, 36 and 48 hours after the initialization of NMMB-MONARCH model at 00 UTC on 19th May 2008.

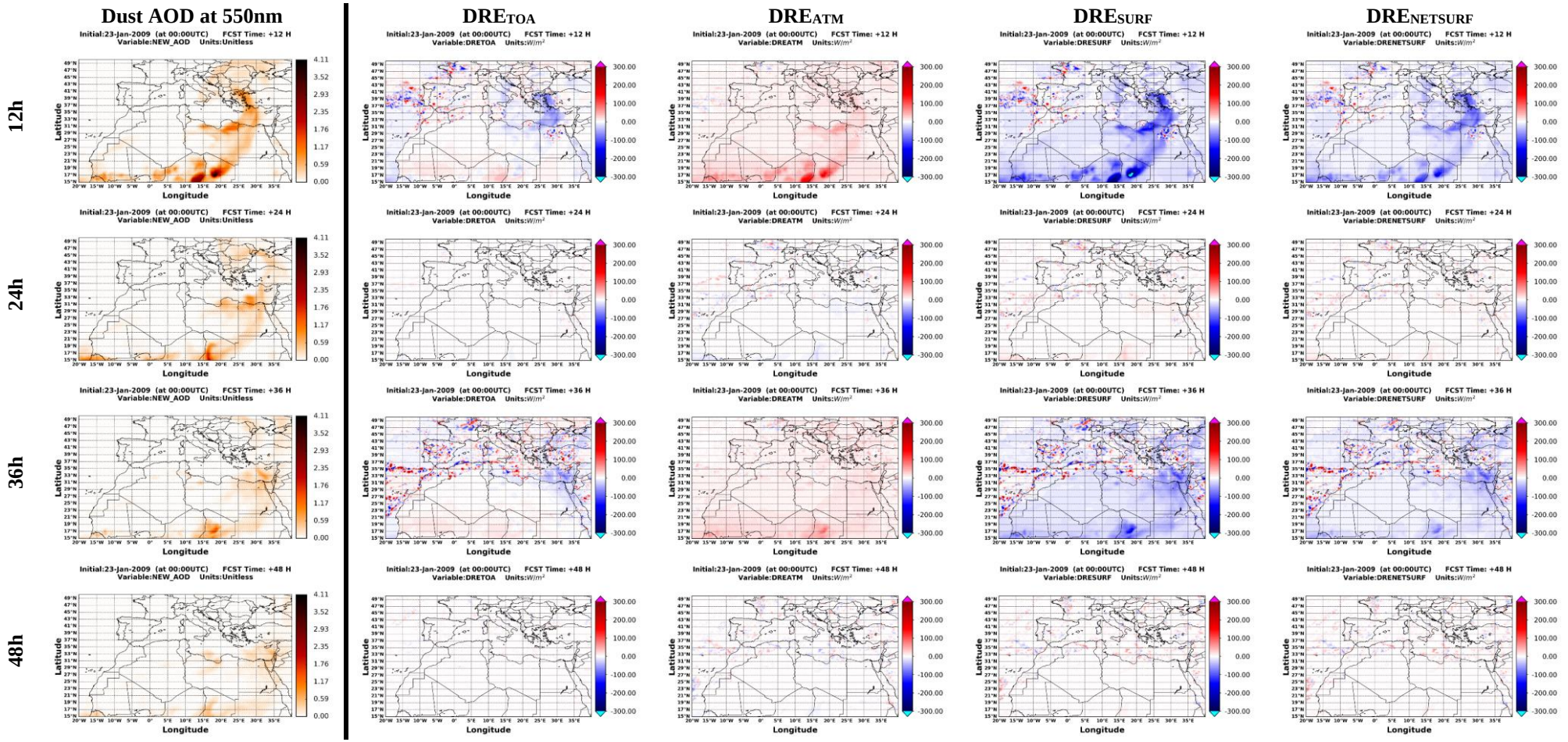

Figure S19: Spatial patterns of the simulated dust AOD_{550nm} and the instantaneous DRE_{TOA}, DRE_{ATM}, DRE_{SURF} and $DRE_{NETSURF}$ values, expressed in Wm^{-2}, at 12, 24, 36 and 48 hours after the initialization of NMMB-MONARCH model at 00 UTC on 23rd January 2009.

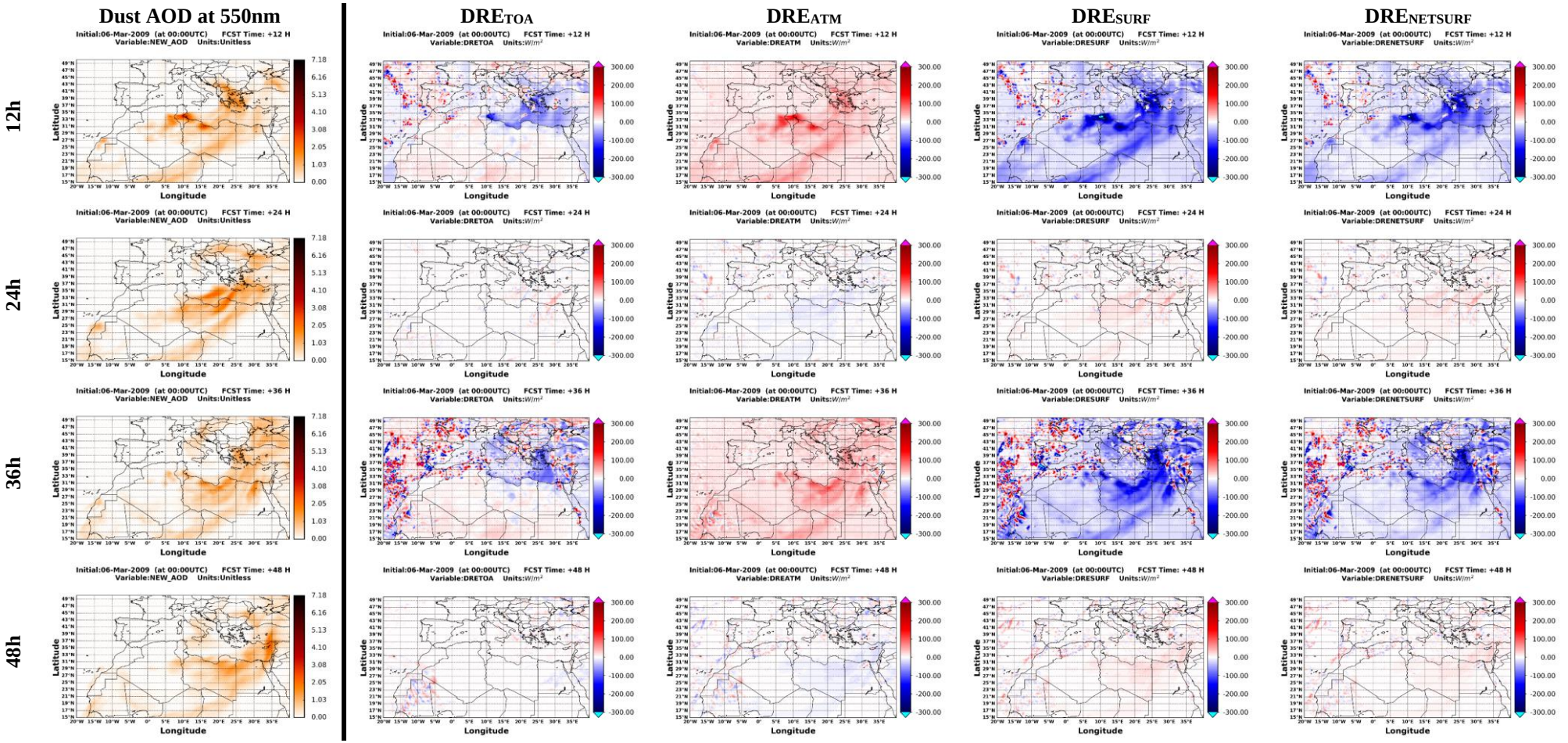

Figure S20: Spatial patterns of the simulated dust AOD_{550nm} and the instantaneous DRE_{TOA}, DRE_{ATM}, DRE_{SURF} and $DRE_{NETSURF}$ values, expressed in Wm^{-2}, at 12, 24, 36 and 48 hours after the initialization of NMMB-MONARCH model at 00 UTC on 6th March 2009.

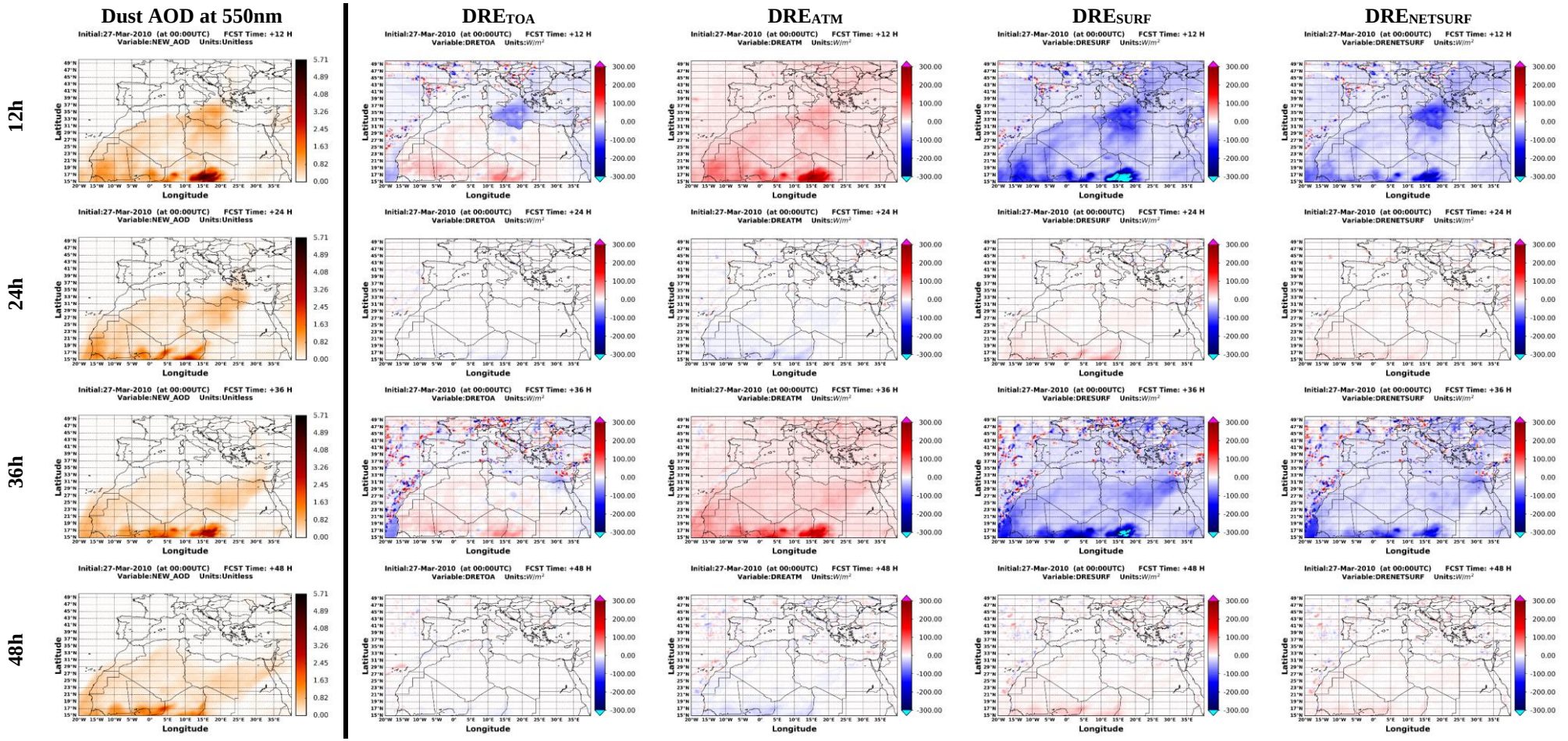

Figure S21: Spatial patterns of the simulated dust AOD_{550nm} and the instantaneous DRE_{TOA}, DRE_{ATM}, DRE_{SURF} and $DRE_{NETSURF}$ values, expressed in Wm^{-2}, at 12, 24, 36 and 48 hours after the initialization of NMMB-MONARCH model at 00 UTC on 27th March 2010.

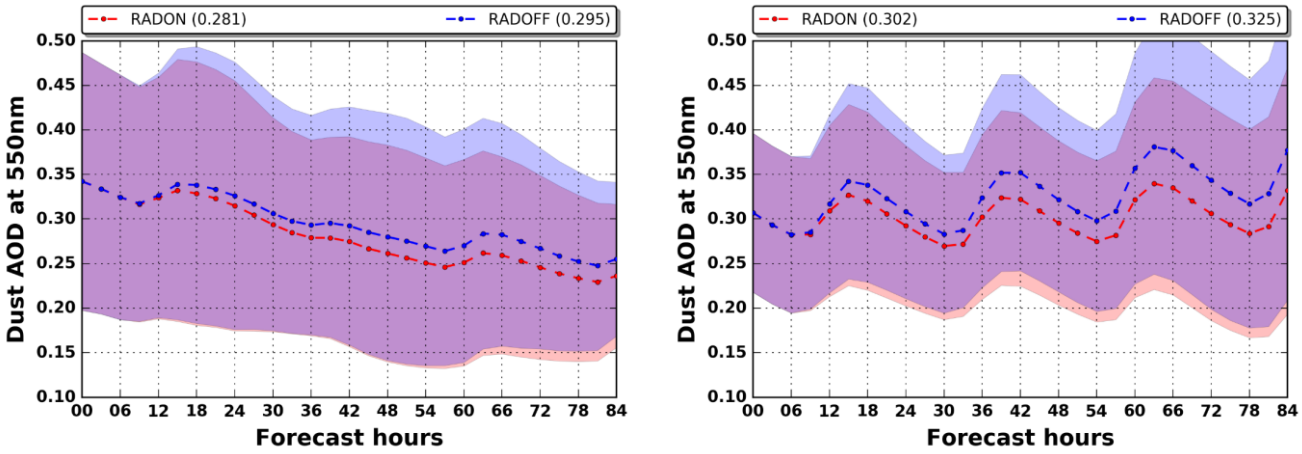

(i) (ii)

Figure S22: Regional dust AOD at 550nm averaged over: (i) the Mediterranean Satellite Domain (MSD) and (ii) the Sahara Desert Domain (SDD). Blue and red curves correspond to the mean values, calculated from the 20 desert dust outbreaks, for the RADOFF and RADON simulations, respectively, and the shaded areas represent the associated standard deviation.

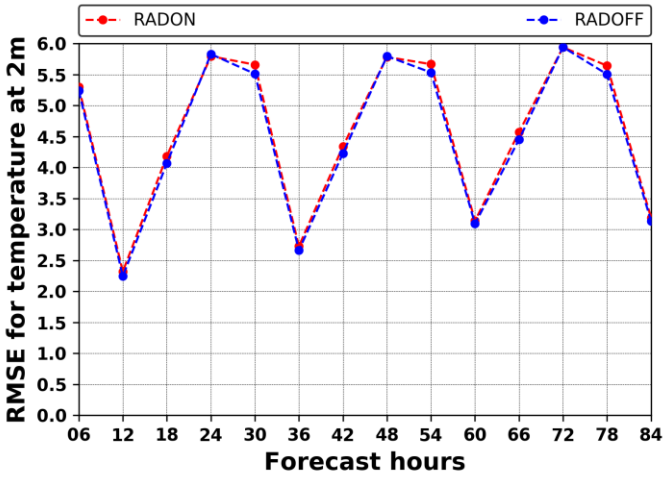

(i)

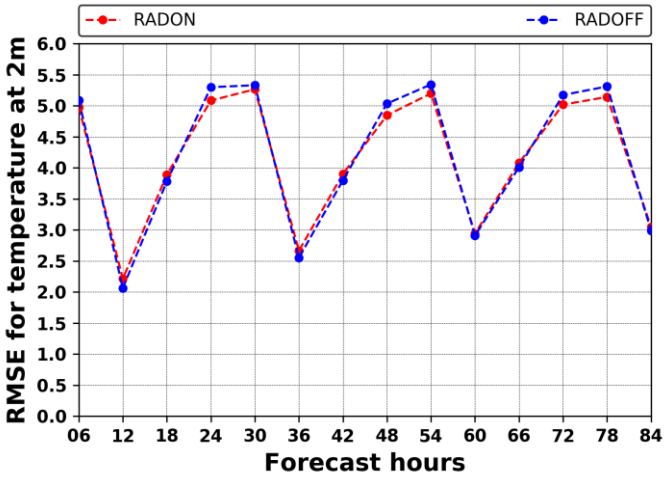

(ii)

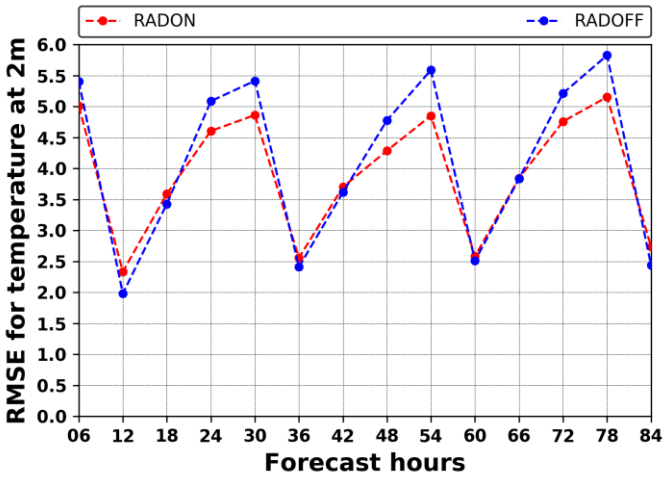

(iii)

Figure S23: Regional root mean square error (RMSE) of temperature at 2 meters between NMMB-MONARCH and FNL, at 1°x1° degrees spatial resolution, calculated over land grid points of the simulation domain (NSD) in which dust AOD at 550 nm is higher/equal than: (i) 0.1, (ii) 0.5 and (iii) 1.0.

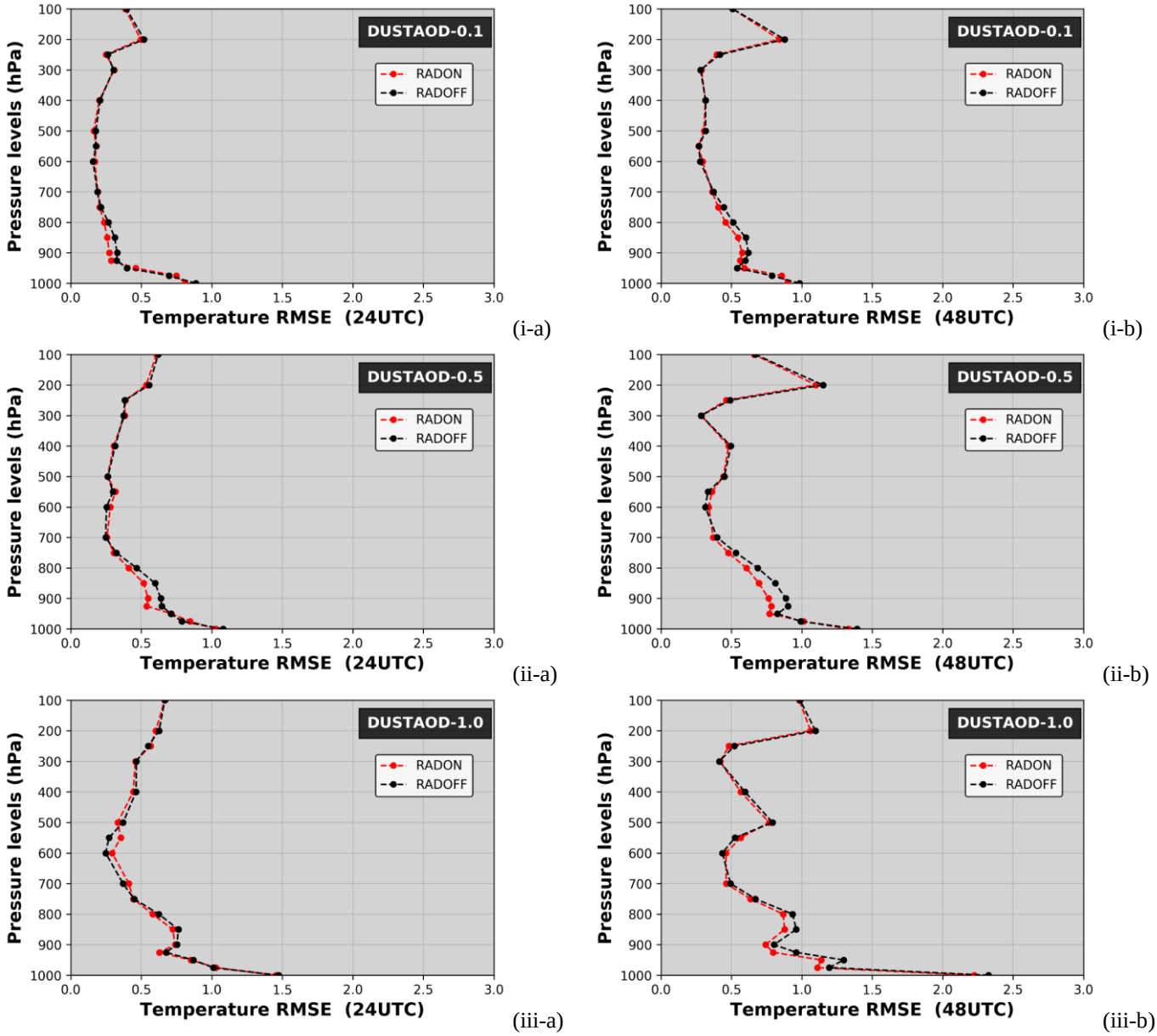

Figure S24: Vertical profiles of the regional temperature root mean square error (RMSE), for RADON-FNL (red curve) and RADOFF-FNL (black curve), calculated from the 20 desert dust outbreaks over grid points (1° x 1° degrees spatial resolution) where the dust AOD at 550 nm is higher/equal than: (i) 0.1, (ii) 0.5 and (iii) 1.0. The obtained results are valid: (a) 24 and (b) 48 hours after the initialization of the forecast period.

Table S1: Minimum and maximum clear sky NET (shortwave plus longwave) DREs, in Wm^{-2}, at grid cell level (geographical distributions) for TOA (second column), ATM (third column), SURF (fourth column) and NETSURF (fifth column), over the 84-h simulation period, for each studied desert dust outbreak (first column).

Date	DRE_{TOA}	DRE_{ATM}	DRE_{SURF}	$DRE_{NETSURF}$
31 July 2001	-81/56	-32/228	-377/48	-211/33
8 May 2002	-141/35	-36/129	-272/37	-257/37
4 April 2003	-113/36	-28/141	-220/35	-201/29
16 July 2003	-143/46	-33/195	-338/50	-261/38
22 February 2004	-127/36	-30/118	-205/32	-191/29
26 March 2004	-117/63	-38/185	-296/46	-196/34
27 January 2005	-113/18	-34/104	-206/44	-165/37
2 March 2005	-162/46	-40/204	-363/48	-271/36
28 July 2005	-99/52	-32/235	-410/38	-231/39
24 February 2006	-120/29	-24/89	-196/31	-183/27
19 March 2006	-133/52	-25/143	-225/29	-211/27
24 February 2007	-110/58	-45/258	-500/61	-258/36
21 April 2007	-103/71	-36/205	-345/63	-190/38
29 May 2007	-83/70	-37/253	-480/66	-258/43
10 April 2008	-87/78	-51/239	-378/78	-180/44
19 May 2008	-159/55	-30/148	-313/41	-295/29
23 January 2009	-124/39	-31/155	-320/43	-197/29
6 March 2009	-184/67	-39/319	-589/46	-337/40
27 March 2010	-91/85	-61/285	-485/83	-258/50
2 August 2012	-161/58	-45/189	-308/58	-290/42

Table S2: Averaged differences (biases), calculated over the 84-h simulation period, between model outputs (RADON/RADOFF) and ground measurements (BSRN) of the downwelling SW radiation at the ground. For each desert dust outbreak (rows), the obtained results are provided for the six BSRN stations (columns) considered in the evaluation analysis. Empty cells correspond to cases where the ground measurements were not totally available throughout the simulation period.

Date	Izana	Cener	Palaiseau	Carpentras	Tamanrasset	Sede Boker
31 July 2001				65.9/86.7	56.0/68.6	
8 May 2002				89.5/124.7	69.2/80.5	
4 April 2003				12.4/22.1	12.4/20.4	42.2/75.5
16 July 2003						
22 February 2004					20.2/26.5	33.9/51.1
26 March 2004				-1.7/14.9	47.7/65.7	61.1/78.7
27 January 2005				10.6/17.9	15.7/23.7	37.0/54.3
2 March 2005				21.4/34.6	30.2/57.6	7.2/37.3
28 July 2005				66.6/63.9	34.1/49.9	6.4/21.7
24 February 2006			35.7/39.2	-3.8/2.3	17.2/20.7	
19 March 2006			-0.2/10.1		21.1/32.1	37.0/56.6
24 February 2007			0.9/1.1	15.7/20.9	15.9/21.2	3.1/12.7
21 April 2007					112.1/137.4	40.9/69.0
29 May 2007			5.8/14.1	86.4/105.4	16.5/26.9	2.7/23.3
10 April 2008			-6.0/-6.4	48.3/57.6	14.1/35.8	30.3/50.5
19 May 2008			31.9/36.9		37.6/68.5	16.6/40.7
23 January 2009				0.2/2.5	11.8/17.1	8.3/18.2
6 March 2009			37.9/54.0		27.0/32.2	-17.8/15.0
27 March 2010	-40.7/-33.1	20.0/19.4	-26.5/-15.1	46.1/55.6	17.8/36.6	64.4/71.8
2 August 2012	-76.7/-11.5	-38.3/-31.8	38.5/51.2	16.2/31.3	-24.9/6.2	2.4/15.0

Table S3: As in Table S2 but for the downwelling LW radiation at the ground.

Date	Izana	Cener	Palaiseau	Carpentras	Tamanrasset	Sede Boker
31 July 2001				-19.1/-19.6	-14.7/-16.2	
8 May 2002				-2.5/-6.6	-17.4/-16.8	
4 April 2003				-21.5/-21.7	-7.1/-7.5	-14.0/-16.7
16 July 2003						
22 February 2004					-2.7/-2.8	-23.6/-25.3
26 March 2004				-16.0/-17.3	-3.2/-5.3	-22.3/-23.4
27 January 2005				-11.6/-11.8	-10.2/-10.6	2.2/-3.6
2 March 2005				2.5/4.7	-4.7/-8.3	-7.5/-8.8
28 July 2005				-25.0/-24.6	-22.7/-24.3	
24 February 2006			-15.0/-15.7	0.8/1.0	-4.8/-4.7	
19 March 2006			2.6/3.7		-11.5/-13.1	
24 February 2007			11.9/12.5	-12.0/-15.9	-3.6/-4.0	-14.0/-15.5
21 April 2007					-8.5/-7.2	6.3/0.7
29 May 2007			-9.4/-8.7	-12.0/-12.3	-21.1/-22.5	11.6/8.4
10 April 2008			14.3/11.8	-11.2/-10.6	-14.2/-17.9	-3.0/-7.2
19 May 2008			-13.9/-9.1		-13.4/-15.4	-7.1/-9.4
23 January 2009				-4.2/-3.7	-1.6/-2.1	-1.2/1.1
6 March 2009			2.4/-0.6		-12.7/-12.1	5.5/3.9
27 March 2010	96.9/95.8	-5.1/0.3	3.6/-0.2	-7.9/-14.4	-22.5/-24.3	-9.0/-8.1
2 August 2012	61.2/51.1	16.2/17.6	-1.7/-1.1	-14.7/-13.3	-4.7/-6.7	-3.4/-2.8